LA-UR-16-29183
Approved for public release; distribution is unlimited.

Title: Validation of MCNP6 Version 1.0 with the ENDF/B-VII.1 Cross Section Library for Plutonium Metals, Oxides, and Solutions on the High Performance Computing Platform Moonlight

Author(s): Chapman, Bryan Scott
Gough, Sean T.

Intended for: Report

Issued: 2016-12-05

Los Alamos
NATIONAL LABORATORY
EST. 1943

Criticality Safety Technical Document
Nuclear Criticality Safety Division

To: NCS File
Through: S. A. Parra, NCS, E585
From: S. T. Gough, NCS, E585
From: B. S. Chapman, NCS, E585
Phone/Fax: 7-3477
7-1629
Email: sgough@lanl.gov
bschapman@lanl.gov
Symbol: NCS-TECH-15-005
Date: 2015-05-12

Validation of MCNP6 Version 1.0 with the ENDF/B-VII.1 Cross Section Library for Plutonium Metals, Oxides, and Solutions on the High Performance Computing Platform Moonlight

1.0 Summary

Nuclear criticality safety analyses are performed for all fissile material systems and operations at facilities that handle fissile material. The nuclear criticality safety analysis establishes the nuclear safety operating limits for fissile material systems and operations. Calculational methods are used to provide an estimate of criticality conditions, and sensitivity analyses are run to determine the margin of subcriticality for all fissile material systems and operations. The computational methods predict the neutronic behavior of the fissile material system or operation of interest. However, the computer code must be validated because certain approximations are inherent in the computer code used, including neutron cross section data and statistical uncertainty.

Validation compares the computational method with benchmark critical experiments to determine any bias that might exist between the calculated results of a given system and the benchmark critical experiment conditions. It is a process that determines and establishes computational method applicability, adequacy, and uncertainty.

This report documents a validation of the MCNP6 Version 1.0 (Reference 2) computer code, on the High-Performance Computing (HPC) platform Moonlight, for operations at Los Alamos National Laboratory (LANL) that involve plutonium metals, oxides, and solutions. The validation is conducted using the ENDF/B-VII.1 continuous energy group cross section library at room temperature (293.6 K). The results are for use by nuclear criticality safety personnel in performing analysis and evaluation of various facility activities involving plutonium materials. Through the selection and validation of appropriate benchmark critical experiments and analysis, this report validates the computational methods for an entire range of normal and abnormal operating conditions involving fissile material. The benchmark critical experiments are modeled as reported in NEA/NCS/DOC (95)03 (Reference 1).

2.0 MCNP6 Verification

The MCNP6 version 1.0 code has been verified on the Moonlight cluster (Reference 3). The HPC platform Moonlight is hosted and maintained by the HPC division. The hardware consists of nodes having two Eight-Core Intel Xeon model E5-2670 processor chips at 2.6 GHz. The operating system is Clustered High Availability Operating System (CHAOS), a Lawrence

Livermore National Laboratory-modified version of RedHat Linux. The input and output files for the benchmark critical experiments modelled are stored in a controlled directory, as documented in Appendix 1.

2.1 MCNP6 Summary

MCNP is a general-purpose Monte Carlo N–Particle code that can be used for neutron, photon, electron, or coupled neutron/photon/electron transport, including the capability to calculate eigenvalues for critical systems. The code treats an arbitrary three-dimensional configuration of materials in geometric cells bounded by first- and second-degree surfaces and fourth-degree elliptical tori.

Pointwise cross section data are used. For neutrons, all reactions given in a particular cross section evaluation (such as ENDF/B-VII.1) are accounted for. Thermal neutrons are described by both the free gas and $S(\alpha,\beta)$ models. For photons, the code accounts for incoherent and coherent scattering, the possibility of fluorescent emission after photoelectric absorption, absorption in pair production with local emission of annihilation radiation, and bremsstrahlung. A continuous-slowing-down model is used for electron transport that includes positrons, k x-rays, and bremsstrahlung, but does not include external or self-induced fields.

Important standard features that make MCNP very versatile and easy to use include a powerful general source, criticality source, and surface source; both geometry and output tally plotters; a rich collection of variance reduction techniques; a flexible tally structure; and an extensive collection of cross section data.

2.2 ENDF/B-VII.1 Cross Section Library

The ENDF/B-VII.1 cross section library at room temperature (293.6 K) is used for the benchmark critical experiment calculations in this validation analysis. A list of the nuclides benchmarked in this evaluation is provided in Table 1. All of these nuclides were identified with the 80c extension in the cases executed for the validation.

Table 1 Library Definitions of Evaluated Nuclides

Element	ZAID	Element	ZAID
Hydrogen	1001	Gallium	31069
Lithium	3006		31071
	3007	Zirconium	40090
Beryllium	4009		40091
Boron	5010		40092
	5011		40094
Carbon	6000		40096
Nitrogen	7014	Molybdenum	42092
	7015		42094
Oxygen	8016		42095
	8017		42096
Sodium	11023		42097
Magnesium	12024		42098
	12025		42100
	12026	Silver	47107

Element	ZAID
Aluminum	13027
Silicon	14028
	14029
	14030
Phosphorus	15031
Sulfur	16032
	16033
	16034
	16036
Chlorine	17035
	17037
Argon	18036
	18038
	18040
Potassium	19039
	19040
	19041
Calcium	20040
	20042
	20043
	20044
	20046
	20048
Titanium	22046
	22047
	22048
	22049
	22050
Vanadium	23050
	23051
Chromium	24050
	24052
	24053
	24054
Manganese	25055
Iron	26054
	26056
	26057
	26058
Cobalt	27059
Nickel	28058
	28060
	28061
	28062
	28064
Copper	29063
	29065
Zinc	30064
	30066
	30067
	30068
	30070

Element	ZAID
	47109
Cadmium	48106
	48108
	48110
	48111
	48112
	48113
	48114
	48116
Tin	50112
	50114
	50115
	50116
	50117
	50118
	50119
	50120
	50122
	50124
Barium	56130
	56132
	56134
	56135
	56136
	56137
	56138
Gadolinium	64152
	64154
	64155
	64156
	64157
	64158
	64160
Tantalum	73181
Tungsten	74182
	74183
	74184
	74186
Lead	82204
	82206
	82207
	82208
Bismuth	83209
Thorium	90232
Uranium	92234
	92235
	92238
Plutonium	94238
	94239
	94240
	94241
	94242
Americium	95241

In addition to the above, several room temperature *S(α,β)* tables are used to model thermal scattering in certain materials, as shown in Table 2.

Table 2 Library Definitions of Evaluated *S*(*α*,*β*) Tables

Material	ZAID	*S(α,β)*
Aluminum	13027	al27.22t
Be Metal	4009	be.20t
BeO	4009	be-o.20t
	8016, 8017, 8018	o-be.20t
Iron	26056	fe56.22t
Graphite	6000, 6012	grph.20t
Light Water	1001	lwtr.20t
Polyethylene	1001	poly.20t
Silicon Dioxide	8016, 14028, 14029	sio2.30t

3.0 Validation Methodology

ANSI/ANS-8.1 (Reference 4) requires that calculational methods used for nuclear criticality safety (e.g., to determine the k_{eff} of a system or derive subcritical limits) be validated to determine the appropriate biases and bias uncertainties for the areas of applicability. The bias and bias uncertainty represent the numerical difference between the results of modeling benchmark critical experiments with a computer code and the measured experimental k_{eff}. These biases may result in either under- or over-predictions of criticality, and the bias may be reported as either positive or negative. A positive bias occurs when the computations tend to report a higher k_{eff} than the benchmark critical experiments (i.e., $k_{eff} > 1.0$), while a negative bias occurs when the calculated results tend to report a lower k_{eff} than the benchmark critical experiments (i.e., $k_{eff} < 1.0$).

Biases (and their associated bias uncertainties) are determined through statistical treatment of the calculated results from benchmark critical experiments. Weighted single sided lower tolerance limits are used for statistical calculations in this validation report when the calculated results are normally distributed. A non-parametric method is used herein when the calculated results are not from a normal distribution.

When performing calculations to assess the subcriticality of a fissile material system or operation, a limit must be established on the calculated k_{eff} to ensure that subcriticality is maintained. This limit is defined for the purposes of this validation as the Upper Subcritical Limit (USL). In this validation, the USL is determined by statistical analysis of the calculated k_{eff} data from the benchmark critical experiments. An additional Margin of Subcriticality (MoS) is added to ensure subcriticality. Also, an additional area of applicability margin (AoA) may be necessary for uncertainties related to interpolation and extrapolation beyond the validated area of applicability.

3.1 Establishment of an Upper Subcritical Limit (USL)

The purpose of a computer code validation is to determine values of k_{eff} that are demonstrated to be subcritical (i.e., at or below the USL) for areas of applicability similar to fissile material systems or operations being analyzed. The USL is defined as follows:

$$USL = 1.0 + Bias – Bias\ Uncertainty – MoS – AoA$$

where:

Bias =	difference between benchmark critical experimental conditions and the calculated results of those experiments.
Bias Uncertainty =	statistical uncertainty in the bias
MoS =	margin of subcriticality (See Section 3.2)
AoA =	additional margin for calculations outside the area of applicability (see Section 3.3)

The bias and its associated bias uncertainty may be represented by one of several statistical methods, as described in Section 3.4).

A k_{eff} calculated by an analysis is then required to meet the following condition:

$$\text{calculated } k_{eff} + 2\sigma \leq USL$$

where σ is the Monte Carlo statistical uncertainty associated with the analysis. Using 2σ provides the 95% confidence level that the Monte Carlo calculated k_{eff} will remain below the USL.

3.2 Margin of Subcriticality

As defined in Section 3.1, the USL explicitly incorporates a margin of subcriticality (MoS), which is required per ANSI/ANS-8.24 (Reference 10). The MoS is an additional administrative margin applied to nuclear criticality safety calculations. Section 6.4 of Reference 10 states that:

> *"A margin of subcriticality shall be applied that is sufficiently large to ensure that calculated conditions will actually be subcritical. The selection of a margin of subcriticality should take into account the sensitivity of the system or process to variations in fissile form, geometry or other physical characteristics. A single margin might not be appropriate over the entire validation applicability."*

The phrase "ensure subcriticality" in ANSI/ANSI 8.24 implies that the analyst should not have any reservations that the condition modeled is actually subcritical. This cannot be done with normal statistical methodologies and therefore relies on an administrative margin to ensure subcriticality.

Reference 11 provides guidance on the selection of an appropriate MoS. However, it is ultimately the responsibility of the analyst to apply the proper MoS for the system being analyzed, and careful consideration needs to be taken when this determination is being made.

3.3 Area of Applicability

The area of applicability determination quantifies parameters potentially important to the computational calculation of k_{eff}. An area of applicability determination should be performed as a part of every calculation performed and compared to the area of applicability of the benchmark critical experiments used for the code validation. This comparison insures that the selected USL

is valid for the calculations being performed. For systems which are outside the validation area of applicability, an area of applicability margin (AoA) may also be warranted, depending on the specific problem being analyzed. The analyst must document and justify any extrapolation beyond the validation area of applicability, including any chosen margin. Guidance for extrapolation may be found in LA-12683 (Reference 5), specifically Appendix E of that report.

3.4 Discussion of Statistical Analysis

The bias and its associated bias uncertainty may be represented by one of several statistical methods depending on whether the data follows a normal distribution. A weighted, single sided lower tolerance limit analysis is used herein when the data has a normal statistical distribution. A weighted, single sided lower tolerance limit is a single lower limit above which a defined fraction of the true population of k_{eff} is expected to lie, with a proscribed confidence and with the defined area of applicability. A lower tolerance limit should be used when there are no apparent trends in the benchmark results.

If the data does not have a normal statistical distribution, a non-parametric statistical treatment must be used. The method used for analysis of data with a non-normal distribution is taken from NUREG/CR-6698 (Reference 9). It should be noted that this approach is more conservative than other methods for dealing with non-normal data distribution, for example calculating a distribution-free confidence interval based on the sign test as presented Reference 6.

3.4.1 Normality Testing of Data

There are several tests which can be performed to determine if data follows a normal distribution. For cases with greater than 50 data points used in establishing the area of applicability, the modified Chi Square test, Kolmogorov-Smirnov test, or Lilliefors test may be utilized. The methodology for these tests can be found in NUREG/CR-4604 (Reference 7) and Natrella (Reference 8).

For the modified Chi Square test, the benchmark critical experiment data are ordered and grouped into classes. For each class, the data range midpoint (m_j) and data point frequency (O_j) are recorded. The method of moments is used to estimate the mean ($\overline{\mu}$) and the variance ($\overline{\sigma}^2$):

$$\overline{\mu} = \sum_{j=1}^{c} \frac{O_j m_j}{n}$$

$$\overline{\sigma}^2 = \left[\sum_{j=1}^{c} \frac{O_j m_j^2}{n} \right] - \overline{\mu}^2$$

where n is the number of benchmark critical experiments and c is the number of classes in which the experimental data are grouped.

The expected values E_j are then computed for a normal distribution with mean $\overline{\mu}$ and variance $\overline{\sigma}^2$. The test statistic is computed using the following:

$$\chi^* = \left[\sum_{j=1}^{c} \frac{O_j^2}{E_j}\right] - n$$

χ^* is compared to $\chi^2_{1-\alpha}(c-k-1)$ obtained from Table A4 of Reference 7, where *k* is the number of unspecified parameters and α is 0.05. If χ^* is less than $\chi^2_{1-\alpha}(c-k-1)$, the hypothesis that the data is from a normal distribution is supported.

For the Kolmogorov-Smirnov test, the empirical cumulative distribution function (cdf) G(x) from the random sample is compared with the hypothesized cdf F*(x). The empirical cdf is a function of x, which equals the fractions of the observations x_i that are less than or equal to x for each x, $-\infty < x < \infty$. The test statistic is calculated as follows:

$$T^* = \sup_x \left|F^*(x) - G(x)\right|$$

The supremum requires comparing F*(x) to G(x) both just before and just after each step in G(x). Both $\left|F^*(x_i) - G(x_i)\right|$ and $\left|F^*(x_i) - G(x_{i-1})\right|$ are calculated and T* is the largest of the absolute differences over all *i*. If T* is less than $w_{1-\alpha}$ (determined from Table A17 in Reference 7), the hypothesis that the data are from a normal distribution is supported.

For the Lilliefors test, the standardized sample values are calculated:

$$z_i = \frac{x_i - \bar{x}}{s}$$

where: x = sample mean
s = sample standard deviation

The test consists of letting F*(z) be the standard normal cdf and then comparing it to the empirical cdf of the z_is, denoted by G(z). The Lilliefors test statistic is the greatest difference between F*(z) and G(z), i.e.:

$$T^* = \sup_z \left|F^*(z) - G(z)\right|$$

T* is the largest of all values $|F^*(z_i) - G(z_i)|$ or $|F^*(z_i) - G(z_{i-1})|$. Values of $F^*(z_i)$ are obtained from Table A3 in Reference 7. The table consists of values for the cumulative standard normal distribution. T* is compared to $w_{1-\alpha}$, obtained from Table A18 of Reference 7. The variable $w_{1-\alpha}$ is dependent on the sample size as well as the desired level of significance. If T* is less than $w_{1-\alpha}$, the data are probably from a normal distribution.

3.4.2 Weighted Single Sided Lower Tolerance Limit

If the benchmark critical experiment results are verified to be part of a normal distribution, a weighted, single sided lower tolerance limit technique may be used to construct a USL for criticality safety. The weighted, single sided lower tolerance limit is calculated with a 95% confidence that 95% of the benchmark data lies above it. Thus, a calculation involving a subcritical system would have a 95% confidence that 95% of all calculations performed on it would yield a result less than the tolerance limit. The weighted, single sided lower tolerance limit is calculated using the method presented in NUREG/CR-6698 (Reference 9). Note that "*This method cannot be used to extrapolate the area of applicability beyond the limits of the validation data*" (Reference 9).

First, take the equation from Section 3.1 where the USL is defined as follows:

$$\text{USL} = 1.0 + \text{Bias} - \text{Bias Uncertainty} - \text{MoS} - \text{AoA}$$

Then, bias is defined as: Bias = $\bar{k}_{eff} - 1$ if $\bar{k}_{eff} < 1$, otherwise Bias = 0. This is done to eliminate any positive, non-conservative bias. Then, with Bias Uncertainty = $K^* S_t$:

$$\text{USL} = \bar{k}_{eff} - K^* S_t - \text{MoS} - \text{AoA}, \ \bar{k}_{eff} < 1 \text{ or}$$

$$\text{USL} = 1 - K^* S_t - \text{MoS} - \text{AoA}, \ \bar{k}_{eff} \geq 1$$

where:
- USL = Maximum subcritical value of k_{eff}
- $\bar{k}_{eff}$ = weighted mean k_{eff} value of the benchmark critical experiments
- K^* = tolerance factor, 2.065 for the 95% confidence level (Reference 9)
- S_t = square root of the pooled variance
- S^2 = variance about the mean
- MoS = margin of subcriticality
- AoA = additional margin for calculations outside the area of applicability (i.e., interpolation within the area of applicability)

and

$$\bar{k}_{eff} = \frac{\sum \frac{1}{\sigma_i^2} k_{eff_i}}{\sum \frac{1}{\sigma_i^2}}$$

$$S^2 = \frac{\left(\frac{1}{n-1}\right) \sum \frac{1}{\sigma_i^2} \left(k_{eff} - \bar{k}_{eff}\right)^2}{\frac{1}{n} \sum \frac{1}{\sigma_i^2}}$$

$$\sigma_i = \sqrt{(\sigma_s^2 + \sigma_e^2)}$$

$$\overline{\sigma}^2 = \frac{n}{\sum \frac{1}{\sigma_i^2}}$$

$$S_t = \sqrt{(S^2 + \overline{\sigma}^2)}$$

where:
- σ_s = Monte Carlo statistical uncertainty associated with calculations that modeled the benchmark critical experiments
- σ_e = experimental uncertainty associated with the benchmark critical experiment
- $\overline{\sigma}^2$ = average uncertainty

The statistical uncertainty, σ_s, is the Monte Carlo standard deviation calculated by the code and reported in the output for each benchmark critical experiment. If available, the experimental uncertainty, σ_e, is determined through rigorous evaluation of each benchmark critical experiment. NEA/NCS/DOC (95)03 documents such evaluations and thus reports an experimental uncertainty.

3.4.3 Non-Parametric Analysis

If the benchmark critical experiment results are not normally distributed, then the data can be analyzed using non-parametric techniques. The method used for this validation is taken from NUREG/CR-6698 (Reference 9). As stated previously, this approach is more conservative than other non-parametric techniques available to determine distribution-free confidence interval. This method results in a determination of the degree of confidence that a fraction of the true population of data lies above the smallest observed value. This determination is calculated as follows:

$$\beta = 1 - \sum_{j=0}^{m-1} \frac{n!}{j!(n-j)!}(1-q)^j \; q^{n-j}$$

where:

- β = level of confidence
- q = the desired population fraction (0.95 for this validation)
- n = the number of data in one data sample
- m = the rank order indexing from the smallest sample to the largest (m=1 for the smallest sample); non-parametric techniques do not require reliance upon distributions but are rather an analysis of ranks
- j = the ranked sample in the sample population being evaluated

As stated in NUREG/CR-6698, for a desired population fraction of 95% and a rank order of 1 (the smallest data sample), the equation simplifies to:

$$\beta = 1 - 0.95^n$$

For a non-parametric set of data, the combination of bias and bias uncertainty is represented by the minimum calculated k_{eff} in the data set, the associated uncertainty, and a non-parametric margin. The USL is then determined as follows:

$$USL = \text{Smallest } k_{eff} \text{ value in the data set} - \sigma_t - NPM - MoS - AoA$$

where:
- σ_t = combined uncertainty corresponding to the smallest k_{eff} value in the data set (i.e., calculational and experimental)
- NPM = non-parametric margin, determined from β
- MoS = margin of subcriticality
- AoA = additional margin for calculations outside the area of applicability

The non-parametric margin is an additional amount subtracted from the lowest data point to account for sample size and non-normal distribution of the data. Recommended values for the non-parametric margin are established in NUREG/CR-6698, Table 2.2.

4.0 Benchmark Experiments

The benchmark critical experiments modeled herein are described below. The chosen benchmark critical experiments comprise 261 individual cases, including 68 plutonium metal cases, 35 plutonium oxide cases, and 158 plutonium nitrate solution cases. These benchmarks were chosen to encompass the range of normal and credible abnormal operating conditions anticipated for systems or processes to which this validation will be applied. The benchmarks were chosen to cover a wide variety of plutonium forms (e.g., Pu metal, PuO_2, $Pu(NO_3)_4$), moderation, homogeneity or heterogeneity, ^{240}Pu content, spectra, and geometry. Note, however, that MCNP6 is a Monte Carlo code and does not employ quadrature, meshes (except for tallies), or cell homogenization. Therefore, it is not a significant concern if certain geometries are not covered in the chosen benchmark critical experiments.

The benchmark critical experiments were taken from the International Handbook of Evaluated Criticality Safety Benchmark Experiments (NEA/NCS/DOC (95)03). A summary of the benchmark critical experiment information is listed in Appendix 2.

4.1 Normalization of k_{eff}

If a critical experiment being modeled was at other than a critical state, (i.e., slightly super or subcritical), NUREG/CR-6698 recommends that the calculated k_{eff} be adjusted. This adjustment is done by normalizing the k_{calc} value to the experimental value. This normalization assumes that the inherent bias in the calculation is not affected by the normalization, which is valid for small differences in k_{eff}. To normalize k_{eff}, the following formula applies:

$$k_{normal} = k_{calc} / k_{exp}$$

The k_{normal} values are presented in Section 4.2 and are used in place of k_{eff} in the subsequent normality testing and determination of the USL.

4.2 Experimental and Calculated Results

The experimental k_{eff} and uncertainty data listed in Table 3 are obtained from Reference 1 for each benchmark critical experiment. Further, the experimental uncertainty is combined with the calculated uncertainty by taking the square root of the sum of the squares to yield a total uncertainty for each benchmark critical experiment. The total uncertainty is used as input to the statistical analysis.

The calculated results shown in Table 3 were produced using MCNP6 with ENDF/B-VII.1 cross sections running on the HPC platform Moonlight. They were run with a minimum of 5,000 neutrons per cycle, skipping the first 25 cycles, and running for 225 total cycles. All of the calculated results meet the Shannon entropy test utilized in MCNP6 to show convergence. The lowest calculated k_{normal} value is highlighted.

Table 3 Experimental and Calculated Results

Benchmark	Calc. k_{eff}	Calc. σ	ANECF (MeV)	EALF (MeV)	Exp. k_{eff}	Exp. σ	k_{normal}	Total σ
pu-comp-inter-001-001	1.0116	0.0002	1.27E-01	2.96E-04	1.0000	0.0110	1.0116	0.0110
pu-comp-mixed-001-001	1.0247	0.0002	1.71E+00	9.70E-01	0.9986	0.0041	1.0262	0.0041
pu-comp-mixed-001-002	1.0283	0.0003	6.30E-01	1.69E-03	1.0000	0.0068	1.0283	0.0068
pu-comp-mixed-001-003	1.0238	0.0003	2.71E-01	3.16E-05	0.9990	0.0067	1.0248	0.0067
pu-comp-mixed-001-004	0.9944	0.0003	2.86E-01	3.85E-05	1.0000	0.0066	0.9944	0.0066
pu-comp-mixed-001-005	1.0089	0.0003	9.95E-02	1.56E-06	0.9989	0.0072	1.0100	0.0072
pu-comp-mixed-002-001	1.0310	0.0003	1.05E+00	5.00E-03	0.9990	0.0046	1.0320	0.0046
pu-comp-mixed-002-002	1.0297	0.0003	1.03E+00	4.32E-03	0.9990	0.0046	1.0307	0.0046
pu-comp-mixed-002-003	1.0249	0.0003	1.01E+00	3.57E-03	0.9990	0.0046	1.0259	0.0046
pu-comp-mixed-002-004	1.0146	0.0003	9.84E-01	2.86E-03	0.9990	0.0046	1.0156	0.0046
pu-comp-mixed-002-005	1.0144	0.0003	9.41E-01	1.93E-03	0.9990	0.0046	1.0154	0.0046
pu-comp-mixed-002-006	1.0254	0.0003	4.36E-01	9.52E-05	1.0000	0.0075	1.0254	0.0075
pu-comp-mixed-002-007	1.0235	0.0003	4.31E-01	8.68E-05	1.0000	0.0075	1.0235	0.0075
pu-comp-mixed-002-008	1.0228	0.0003	4.21E-01	7.03E-05	1.0000	0.0075	1.0228	0.0075
pu-comp-mixed-002-009	1.0230	0.0003	4.10E-01	5.88E-05	1.0000	0.0075	1.0230	0.0075
pu-comp-mixed-002-010	1.0324	0.0003	1.83E-01	4.24E-06	1.0000	0.0073	1.0324	0.0073
pu-comp-mixed-002-011	1.0299	0.0003	1.86E-01	4.65E-06	1.0000	0.0073	1.0299	0.0073
pu-comp-mixed-002-012	1.0302	0.0003	1.91E-01	5.28E-06	1.0000	0.0073	1.0302	0.0073
pu-comp-mixed-002-013	1.0276	0.0003	1.93E-01	5.58E-06	1.0000	0.0073	1.0276	0.0073
pu-comp-mixed-002-014	1.0314	0.0003	1.94E-01	5.71E-06	1.0000	0.0073	1.0314	0.0073
pu-comp-mixed-002-015	1.0297	0.0003	1.94E-01	5.68E-06	1.0000	0.0073	1.0297	0.0073
pu-comp-mixed-002-016	1.0260	0.0003	1.91E-01	5.28E-06	1.0000	0.0073	1.0260	0.0073
pu-comp-mixed-002-017	1.0073	0.0003	1.94E-01	5.07E-06	0.9988	0.0055	1.0085	0.0055
pu-comp-mixed-002-018	1.0118	0.0003	2.02E-01	6.32E-06	0.9988	0.0055	1.0130	0.0055
pu-comp-mixed-002-019	1.0109	0.0003	2.04E-01	6.63E-06	0.9988	0.0055	1.0121	0.0055
pu-comp-mixed-002-020	1.0108	0.0003	2.05E-01	6.83E-06	0.9988	0.0055	1.0120	0.0055
pu-comp-mixed-002-021	1.0115	0.0003	2.05E-01	6.85E-06	0.9988	0.0055	1.0127	0.0055
pu-comp-mixed-002-022	1.0153	0.0003	2.04E-01	6.58E-06	0.9988	0.0055	1.0165	0.0055
pu-comp-mixed-002-023	1.0064	0.0003	7.69E-02	7.08E-07	1.0000	0.0068	1.0064	0.0068
pu-comp-mixed-002-024	1.0079	0.0003	7.72E-02	7.20E-07	1.0000	0.0068	1.0079	0.0068
pu-comp-mixed-002-025	1.0076	0.0003	7.74E-02	7.30E-07	1.0000	0.0068	1.0076	0.0068
pu-comp-mixed-002-026	1.0089	0.0003	7.78E-02	7.38E-07	1.0000	0.0068	1.0089	0.0068
pu-comp-mixed-002-027	1.0093	0.0004	7.81E-02	7.47E-07	1.0000	0.0068	1.0093	0.0068
pu-comp-mixed-002-028	1.0092	0.0003	7.80E-02	7.51E-07	1.0000	0.0068	1.0092	0.0068
pu-comp-mixed-002-029	1.0097	0.0003	7.84E-02	7.59E-07	1.0000	0.0068	1.0097	0.0068

Benchmark	Calc. k_{eff}	Calc. σ	ANECF (MeV)	EALF (MeV)	Exp. k_{eff}	Exp. σ	k_{normal}	Total σ
pu-met-fast-001-001	1.0007	0.0006	1.91E+00	1.25E+00	1.0000	0.0020	1.0007	0.0021
pu-met-fast-002-001	1.0004	0.0006	1.92E+00	1.27E+00	1.0000	0.0020	1.0004	0.0021
pu-met-fast-003-103	0.9990	0.0003	1.89E+00	1.24E+00	1.0000	0.0030	0.9990	0.0030
pu-met-fast-005-001	1.0002	0.0006	1.68E+00	1.01E+00	1.0000	0.0013	1.0002	0.0014
pu-met-fast-006-001	1.0010	0.0008	1.90E+00	1.06E+00	1.0000	0.0030	1.0010	0.0031
pu-met-fast-008-001	0.9988	0.0007	1.78E+00	1.07E+00	1.0000	0.0006	0.9988	0.0009
pu-met-fast-009-001	1.0070	0.0006	1.80E+00	1.14E+00	1.0000	0.0027	1.0070	0.0028
pu-met-fast-010-001	1.0003	0.0007	1.89E+00	1.17E+00	1.0000	0.0018	1.0003	0.0019
pu-met-fast-011-001	1.0006	0.0007	1.52E+00	8.21E-02	1.0000	0.0010	1.0006	0.0012
pu-met-fast-012-001	1.0028	0.0007	1.80E+00	9.51E-01	1.0009	0.0021	1.0019	0.0022
pu-met-fast-013-001	1.0084	0.0007	1.49E+00	7.84E-01	1.0034	0.0023	1.0050	0.0024
pu-met-fast-014-001	1.0076	0.0006	1.52E+00	7.91E-01	1.0037	0.0031	1.0039	0.0032
pu-met-fast-015-001	1.0010	0.0006	1.63E+00	9.61E-01	1.0041	0.0026	0.9969	0.0027
pu-met-fast-016-001	1.0174	0.0001	1.28E+00	1.12E-02	0.9974	0.0042	1.0200	0.0042
pu-met-fast-016-002	1.0070	0.0001	1.25E+00	8.04E-03	1.0000	0.0038	1.0070	0.0038
pu-met-fast-016-003	1.0050	0.0001	1.25E+00	7.76E-03	1.0000	0.0033	1.0050	0.0033
pu-met-fast-016-004	1.0045	0.0001	1.24E+00	7.53E-03	1.0000	0.0030	1.0045	0.0030
pu-met-fast-016-005	1.0042	0.0001	1.24E+00	7.40E-03	1.0000	0.0034	1.0042	0.0034
pu-met-fast-016-006	1.0067	0.0001	1.24E+00	7.37E-03	1.0000	0.0032	1.0067	0.0032
pu-met-fast-018-001	0.9995	0.0007	1.67E+00	9.10E-01	1.0000	0.0030	0.9995	0.0031
pu-met-fast-019-001	1.0010	0.0007	1.62E+00	7.72E-01	0.9992	0.0015	1.0018	0.0016
pu-met-fast-020-001	0.9982	0.0006	1.88E+00	1.13E+00	0.9993	0.0017	0.9989	0.0018
pu-met-fast-021-001	1.0045	0.0001	1.66E+00	7.80E-01	1.0000	0.0026	1.0045	0.0026
pu-met-fast-021-002	0.9935	0.0001	1.67E+00	8.66E-01	1.0000	0.0026	0.9935	0.0026
pu-met-fast-022-001	0.9987	0.0006	1.89E+00	1.24E+00	1.0000	0.0021	0.9987	0.0022
pu-met-fast-023-001	1.0002	0.0006	1.80E+00	1.14E+00	1.0000	0.0022	1.0002	0.0023
pu-met-fast-024-001	1.0027	0.0006	1.74E+00	6.35E-01	1.0000	0.0022	1.0027	0.0023
pu-met-fast-025-001	0.9994	0.0006	1.84E+00	1.19E+00	1.0000	0.0022	0.9994	0.0023
pu-met-fast-026-001	0.9990	0.0006	1.74E+00	1.09E+00	1.0000	0.0026	0.9990	0.0027
pu-met-fast-027-001	1.0031	0.0008	1.47E+00	7.17E-02	1.0000	0.0024	1.0031	0.0025
pu-met-fast-028-001	0.9992	0.0006	1.72E+00	1.07E+00	1.0000	0.0024	0.9992	0.0025
pu-met-fast-029-001	0.9955	0.0006	1.92E+00	1.25E+00	1.0000	0.0022	0.9955	0.0023
pu-met-fast-030-001	1.0029	0.0006	1.81E+00	1.14E+00	1.0000	0.0023	1.0029	0.0024
pu-met-fast-031-001	1.0045	0.0007	1.60E+00	1.85E-01	1.0000	0.0023	1.0045	0.0024
pu-met-fast-032-001	0.9983	0.0006	1.82E+00	1.17E+00	1.0000	0.0022	0.9983	0.0023
pu-met-fast-035-001	0.9981	0.0006	1.83E+00	1.18E+00	1.0000	0.0016	0.9981	0.0017
pu-met-fast-036-001	1.0065	0.0001	1.72E+00	6.22E-01	1.0000	0.0031	1.0065	0.0031
pu-met-fast-038-001	1.0026	0.0001	1.55E+00	5.02E-01	1.0007	0.0019	1.0019	0.0019
pu-met-fast-039-001	**0.9922**	**0.0001**	**1.81E+00**	**1.16E+00**	**1.0000**	**0.0022**	**0.9922**	**0.0022**
pu-met-fast-040-001	0.9967	0.0001	1.79E+00	1.15E+00	1.0000	0.0038	0.9967	0.0038
pu-met-fast-041-001	1.0056	0.0001	1.94E+00	1.10E+00	1.0000	0.0016	1.0056	0.0016
pu-met-fast-042-001	1.0198	0.0008	1.43E+00	5.29E-02	1.0004	0.0077	1.0194	0.0077
pu-met-fast-042-002	1.0133	0.0008	1.46E+00	7.12E-02	1.0007	0.0074	1.0126	0.0074
pu-met-fast-042-003	1.0119	0.0008	1.48E+00	8.80E-02	1.0013	0.0080	1.0105	0.0080
pu-met-fast-042-004	1.0100	0.0007	1.50E+00	1.07E-01	1.0026	0.0080	1.0074	0.0080
pu-met-fast-042-005	1.0100	0.0007	1.52E+00	1.21E-01	1.0013	0.0080	1.0087	0.0080
pu-met-fast-042-006	1.0078	0.0008	1.52E+00	1.39E-01	1.0015	0.0079	1.0063	0.0079
pu-met-fast-042-007	1.0075	0.0008	1.53E+00	1.53E-01	1.0006	0.0075	1.0069	0.0075
pu-met-fast-042-008	1.0111	0.0008	1.53E+00	1.57E-01	1.0019	0.0080	1.0092	0.0080
pu-met-fast-042-009	1.0129	0.0007	1.54E+00	1.73E-01	1.0019	0.0073	1.0109	0.0073
pu-met-fast-042-010	1.0148	0.0007	1.54E+00	1.75E-01	1.0015	0.0079	1.0132	0.0079
pu-met-fast-042-011	1.0116	0.0008	1.55E+00	1.86E-01	1.0010	0.0078	1.0105	0.0078
pu-met-fast-042-012	1.0111	0.0007	1.55E+00	1.93E-01	1.0016	0.0076	1.0095	0.0076
pu-met-fast-042-013	1.0112	0.0008	1.55E+00	2.03E-01	1.0016	0.0074	1.0096	0.0074
pu-met-fast-042-014	1.0120	0.0007	1.56E+00	2.08E-01	1.0016	0.0078	1.0104	0.0078
pu-met-fast-042-015	1.0127	0.0008	1.56E+00	2.17E-01	1.0014	0.0076	1.0113	0.0076
pu-met-fast-044-001	1.0005	0.0001	1.65E+00	4.00E-01	0.9977	0.0021	1.0028	0.0021
pu-met-fast-044-002	1.0000	0.0001	1.65E+00	3.16E-01	0.9980	0.0022	1.0020	0.0022
pu-met-fast-044-003	0.9994	0.0001	1.66E+00	4.52E-01	0.9977	0.0021	1.0017	0.0021
pu-met-fast-044-004	1.0000	0.0001	1.60E+00	1.89E-01	0.9978	0.0026	1.0022	0.0026
pu-met-fast-044-005	0.9991	0.0001	1.64E+00	2.84E-01	0.9977	0.0024	1.0014	0.0024
pu-met-fast-045-001	1.0018	0.0005	1.60E+00	8.54E-01	1.0000	0.0047	1.0018	0.0047

Benchmark	Calc. k_{eff}	Calc. σ	ANECF (MeV)	EALF (MeV)	Exp. k_{eff}	Exp. σ	k_{normal}	Total σ
pu-met-fast-045-002	1.0068	0.0007	1.60E+00	8.90E-01	1.0000	0.0046	1.0068	0.0047
pu-met-fast-045-003	1.0054	0.0005	1.62E+00	9.22E-01	1.0000	0.0044	1.0054	0.0044
pu-met-fast-045-004	1.0050	0.0007	1.64E+00	8.96E-01	1.0000	0.0046	1.0050	0.0046
pu-met-fast-045-005	1.0081	0.0007	1.68E+00	9.32E-01	1.0000	0.0045	1.0081	0.0045
pu-met-fast-045-006	1.0059	0.0007	1.65E+00	8.11E-01	1.0000	0.0049	1.0059	0.0049
pu-met-fast-045-007	1.0064	0.0005	1.62E+00	7.43E-01	1.0000	0.0050	1.0064	0.0050
pu-sol-therm-001-001	1.0056	0.0009	1.30E-02	8.67E-08	1.0000	0.0050	1.0056	0.0051
pu-sol-therm-001-002	1.0076	0.0009	1.72E-02	1.09E-07	1.0000	0.0050	1.0076	0.0051
pu-sol-therm-001-003	1.0096	0.0009	2.14E-02	1.32E-07	1.0000	0.0050	1.0096	0.0051
pu-sol-therm-001-004	1.0049	0.0009	2.40E-02	1.48E-07	1.0000	0.0050	1.0049	0.0051
pu-sol-therm-001-005	1.0093	0.0010	2.49E-02	1.56E-07	1.0000	0.0050	1.0093	0.0051
pu-sol-therm-001-006	1.0116	0.0009	4.84E-02	3.42E-07	1.0000	0.0050	1.0116	0.0051
pu-sol-therm-002-001	1.0037	0.0008	9.06E-03	6.99E-08	1.0000	0.0047	1.0037	0.0048
pu-sol-therm-002-002	1.0043	0.0009	9.46E-03	7.14E-08	1.0000	0.0047	1.0043	0.0048
pu-sol-therm-002-003	1.0040	0.0008	1.06E-02	7.64E-08	1.0000	0.0047	1.0040	0.0048
pu-sol-therm-002-004	1.0058	0.0008	1.11E-02	7.94E-08	1.0000	0.0047	1.0058	0.0048
pu-sol-therm-002-005	1.0091	0.0009	1.20E-02	8.32E-08	1.0000	0.0047	1.0091	0.0048
pu-sol-therm-002-006	1.0025	0.0009	1.33E-02	9.13E-08	1.0000	0.0047	1.0025	0.0048
pu-sol-therm-002-007	1.0090	0.0009	1.45E-02	9.83E-08	1.0000	0.0047	1.0090	0.0048
pu-sol-therm-003-001	1.0019	0.0007	6.35E-03	5.71E-08	1.0000	0.0047	1.0019	0.0048
pu-sol-therm-003-002	1.0029	0.0008	6.98E-03	5.85E-08	1.0000	0.0047	1.0029	0.0048
pu-sol-therm-003-003	1.0044	0.0009	7.29E-03	6.10E-08	1.0000	0.0047	1.0044	0.0048
pu-sol-therm-003-004	1.0048	0.0009	7.12E-03	6.13E-08	1.0000	0.0047	1.0048	0.0048
pu-sol-therm-003-005	1.0047	0.0009	7.71E-03	6.40E-08	1.0000	0.0047	1.0047	0.0048
pu-sol-therm-003-006	1.0060	0.0008	8.53E-03	6.80E-08	1.0000	0.0047	1.0060	0.0048
pu-sol-therm-003-007	1.0068	0.0001	6.80E-03	5.81E-08	1.0000	0.0047	1.0068	0.0047
pu-sol-therm-003-008	1.0055	0.0001	7.00E-03	5.91E-08	1.0000	0.0047	1.0055	0.0047
pu-sol-therm-004-001	1.0028	0.0008	4.97E-03	5.22E-08	1.0000	0.0047	1.0028	0.0048
pu-sol-therm-004-002	0.9987	0.0007	5.20E-03	5.30E-08	1.0000	0.0047	0.9987	0.0048
pu-sol-therm-004-003	1.0021	0.0008	5.39E-03	5.38E-08	1.0000	0.0047	1.0021	0.0048
pu-sol-therm-004-004	0.9971	0.0008	5.74E-03	5.50E-08	1.0000	0.0047	0.9971	0.0048
pu-sol-therm-004-005	1.0013	0.0008	5.33E-03	5.35E-08	1.0000	0.0047	1.0013	0.0048
pu-sol-therm-004-006	1.0001	0.0008	5.80E-03	5.40E-08	1.0000	0.0047	1.0001	0.0048
pu-sol-therm-004-007	1.0040	0.0009	5.83E-03	5.48E-08	1.0000	0.0047	1.0040	0.0048
pu-sol-therm-004-008	1.0010	0.0008	5.95E-03	5.54E-08	1.0000	0.0047	1.0010	0.0048
pu-sol-therm-004-009	0.9992	0.0008	6.25E-03	5.75E-08	1.0000	0.0047	0.9992	0.0048
pu-sol-therm-004-010	1.0041	0.0008	7.49E-03	6.20E-08	1.0000	0.0047	1.0041	0.0048
pu-sol-therm-004-011	1.0008	0.0008	8.10E-03	6.69E-08	1.0000	0.0047	1.0008	0.0048
pu-sol-therm-004-012	1.0012	0.0007	5.76E-03	5.48E-08	1.0000	0.0047	1.0012	0.0048
pu-sol-therm-004-013	1.0006	0.0008	5.80E-03	5.48E-08	1.0000	0.0047	1.0006	0.0048
pu-sol-therm-005-001	1.0027	0.0008	5.94E-03	5.45E-08	1.0000	0.0047	1.0027	0.0048
pu-sol-therm-005-002	1.0029	0.0008	5.89E-03	5.55E-08	1.0000	0.0047	1.0029	0.0048
pu-sol-therm-005-003	1.0034	0.0008	6.21E-03	5.67E-08	1.0000	0.0047	1.0034	0.0048
pu-sol-therm-005-004	1.0042	0.0008	6.70E-03	5.90E-08	1.0000	0.0047	1.0042	0.0048
pu-sol-therm-005-005	1.0069	0.0008	7.59E-03	6.16E-08	1.0000	0.0047	1.0069	0.0048
pu-sol-therm-005-006	1.0060	0.0008	7.72E-03	6.48E-08	1.0000	0.0047	1.0060	0.0048
pu-sol-therm-005-007	1.0042	0.0008	8.72E-03	6.80E-08	1.0000	0.0047	1.0042	0.0048
pu-sol-therm-005-008	0.9989	0.0008	6.14E-03	5.57E-08	1.0000	0.0047	0.9989	0.0048
pu-sol-therm-005-009	1.0020	0.0008	6.30E-03	5.68E-08	1.0000	0.0047	1.0020	0.0048
pu-sol-therm-006-001	1.0009	0.0008	5.09E-03	5.14E-08	1.0000	0.0035	1.0009	0.0036
pu-sol-therm-006-002	1.0011	0.0007	5.12E-03	5.25E-08	1.0000	0.0035	1.0011	0.0036
pu-sol-therm-006-003	1.0007	0.0008	5.59E-03	5.42E-08	1.0000	0.0035	1.0007	0.0036
pu-sol-therm-007-002	1.0091	0.0001	4.07E-02	2.70E-07	1.0000	0.0047	1.0091	0.0047
pu-sol-therm-007-003	1.0034	0.0001	3.92E-02	2.56E-07	1.0000	0.0047	1.0034	0.0047
pu-sol-therm-007-005	1.0091	0.0001	1.75E-02	1.10E-07	1.0000	0.0047	1.0091	0.0047
pu-sol-therm-007-006	1.0030	0.0001	1.79E-02	1.12E-07	1.0000	0.0047	1.0030	0.0047
pu-sol-therm-007-007	1.0054	0.0001	1.77E-02	1.11E-07	1.0000	0.0047	1.0054	0.0047
pu-sol-therm-007-008	0.9988	0.0001	1.82E-02	1.13E-07	1.0000	0.0047	0.9988	0.0047
pu-sol-therm-007-009	0.9971	0.0001	1.81E-02	1.13E-07	1.0000	0.0047	0.9971	0.0047
pu-sol-therm-007-010	1.0009	0.0001	1.66E-02	1.05E-07	1.0000	0.0047	1.0009	0.0047
pu-sol-therm-009-003	1.0192	0.0001	2.58E-03	4.05E-08	1.0000	0.0033	1.0192	0.0033
pu-sol-therm-010-001	1.0180	0.0001	1.69E-02	1.08E-07	1.0000	0.0048	1.0180	0.0048

Benchmark	Calc. k_{eff}	Calc. σ	ANECF (MeV)	EALF (MeV)	Exp. k_{eff}	Exp. σ	k_{normal}	Total σ
pu-sol-therm-010-002	1.0146	0.0001	1.30E-02	8.77E-08	1.0000	0.0048	1.0146	0.0048
pu-sol-therm-010-003	1.0083	0.0001	9.88E-03	7.27E-08	1.0000	0.0048	1.0083	0.0048
pu-sol-therm-010-004	1.0126	0.0001	1.00E-02	7.41E-08	1.0000	0.0048	1.0126	0.0048
pu-sol-therm-010-005	1.0107	0.0001	8.83E-03	6.87E-08	1.0000	0.0048	1.0107	0.0048
pu-sol-therm-010-006	1.0094	0.0001	8.76E-03	6.76E-08	1.0000	0.0048	1.0094	0.0048
pu-sol-therm-010-007	1.0025	0.0001	8.13E-03	6.54E-08	1.0000	0.0048	1.0025	0.0048
pu-sol-therm-010-008	1.0040	0.0001	7.52E-03	6.30E-08	1.0000	0.0048	1.0040	0.0048
pu-sol-therm-010-009	1.0147	0.0001	1.14E-02	7.99E-08	1.0000	0.0048	1.0147	0.0048
pu-sol-therm-010-010	1.0027	0.0001	9.11E-03	6.92E-08	1.0000	0.0048	1.0027	0.0048
pu-sol-therm-010-011	1.0099	0.0001	8.96E-03	6.85E-08	1.0000	0.0048	1.0099	0.0048
pu-sol-therm-010-012	1.0097	0.0001	8.01E-03	6.43E-08	1.0000	0.0048	1.0097	0.0048
pu-sol-therm-010-013	1.0160	0.0001	6.96E-03	5.96E-08	1.0000	0.0048	1.0160	0.0048
pu-sol-therm-010-014	1.0096	0.0001	6.13E-03	5.60E-08	1.0000	0.0048	1.0096	0.0048
pu-sol-therm-011-161	1.0101	0.0001	7.65E-03	6.23E-08	1.0000	0.0052	1.0101	0.0052
pu-sol-therm-011-162	1.0147	0.0001	7.91E-03	6.35E-08	1.0000	0.0052	1.0147	0.0052
pu-sol-therm-011-163	1.0168	0.0001	8.38E-03	6.59E-08	1.0000	0.0052	1.0168	0.0052
pu-sol-therm-011-164	1.0090	0.0001	8.54E-03	6.65E-08	1.0000	0.0052	1.0090	0.0052
pu-sol-therm-011-165	1.0064	0.0001	9.90E-03	7.39E-08	1.0000	0.0052	1.0064	0.0052
pu-sol-therm-011-181	0.9944	0.0001	5.17E-03	5.11E-08	1.0000	0.0052	0.9944	0.0052
pu-sol-therm-011-182	1.0003	0.0001	5.35E-03	5.21E-08	1.0000	0.0052	1.0003	0.0052
pu-sol-therm-011-183	0.9970	0.0001	5.36E-03	5.20E-08	1.0000	0.0052	0.9970	0.0052
pu-sol-therm-011-184	0.9937	0.0001	5.62E-03	5.33E-08	1.0000	0.0052	0.9937	0.0052
pu-sol-therm-011-185	1.0035	0.0001	5.86E-03	5.46E-08	1.0000	0.0052	1.0035	0.0052
pu-sol-therm-011-186	1.0005	0.0001	6.56E-03	5.83E-08	1.0000	0.0052	1.0005	0.0052
pu-sol-therm-011-187	0.9996	0.0001	5.57E-03	5.31E-08	1.0000	0.0052	0.9996	0.0052
pu-sol-therm-012-001	1.0055	0.0001	4.75E-03	4.74E-08	1.0000	0.0043	1.0055	0.0043
pu-sol-therm-012-002	1.0059	0.0001	4.36E-03	4.58E-08	1.0000	0.0043	1.0059	0.0043
pu-sol-therm-012-003	1.0071	0.0001	4.16E-03	4.51E-08	1.0000	0.0058	1.0071	0.0058
pu-sol-therm-012-004	1.0077	0.0001	3.78E-03	4.36E-08	1.0000	0.0058	1.0077	0.0058
pu-sol-therm-012-005	1.0098	0.0001	3.49E-03	4.25E-08	1.0000	0.0058	1.0098	0.0058
pu-sol-therm-012-006	1.0065	0.0001	2.22E-02	1.30E-07	1.0000	0.0007	1.0065	0.0007
pu-sol-therm-012-007	1.0052	0.0001	1.77E-02	1.05E-07	1.0000	0.0013	1.0052	0.0013
pu-sol-therm-012-008	1.0042	0.0001	1.14E-02	7.45E-08	1.0000	0.0013	1.0042	0.0013
pu-sol-therm-012-009	1.0100	0.0001	7.22E-03	5.69E-08	1.0000	0.0043	1.0100	0.0043
pu-sol-therm-012-010	1.0039	0.0001	6.28E-03	5.30E-08	1.0000	0.0043	1.0039	0.0043
pu-sol-therm-012-011	1.0065	0.0001	5.17E-03	4.88E-08	1.0000	0.0043	1.0065	0.0043
pu-sol-therm-012-012	1.0068	0.0001	4.80E-03	4.74E-08	1.0000	0.0043	1.0068	0.0043
pu-sol-therm-012-013	1.0096	0.0001	3.50E-03	4.25E-08	1.0000	0.0058	1.0096	0.0058
pu-sol-therm-018-001	1.0082	0.0001	3.36E-02	1.65E-07	1.0000	0.0034	1.0082	0.0034
pu-sol-therm-018-002	1.0117	0.0001	2.72E-02	1.29E-07	1.0000	0.0034	1.0117	0.0034
pu-sol-therm-018-003	1.0094	0.0001	2.30E-02	1.08E-07	1.0000	0.0032	1.0094	0.0032
pu-sol-therm-018-004	1.0077	0.0001	1.97E-02	9.35E-08	1.0000	0.0030	1.0077	0.0030
pu-sol-therm-018-005	1.0064	0.0001	1.74E-02	8.39E-08	1.0000	0.0030	1.0064	0.0030
pu-sol-therm-018-006	1.0045	0.0001	1.49E-02	7.47E-08	1.0000	0.0031	1.0045	0.0031
pu-sol-therm-018-007	1.0041	0.0001	1.29E-02	6.75E-08	1.0000	0.0032	1.0041	0.0032
pu-sol-therm-018-008	1.0036	0.0001	1.08E-02	6.04E-08	1.0000	0.0033	1.0036	0.0033
pu-sol-therm-018-009	1.0021	0.0001	9.49E-03	5.60E-08	1.0000	0.0034	1.0021	0.0034
pu-sol-therm-022-001	0.9996	0.0001	3.26E-02	2.06E-07	1.0000	0.0020	0.9996	0.0020
pu-sol-therm-022-002	1.0022	0.0001	2.15E-02	1.29E-07	1.0000	0.0016	1.0022	0.0016
pu-sol-therm-022-003	1.0008	0.0001	1.28E-02	8.23E-08	1.0000	0.0015	1.0008	0.0015
pu-sol-therm-022-004	1.0015	0.0001	1.07E-02	7.24E-08	1.0000	0.0017	1.0015	0.0017
pu-sol-therm-022-005	1.0025	0.0001	8.74E-03	6.38E-08	1.0000	0.0019	1.0025	0.0019
pu-sol-therm-022-006	1.0025	0.0001	7.77E-03	5.99E-08	1.0000	0.0021	1.0025	0.0021
pu-sol-therm-022-007	1.0043	0.0001	7.26E-03	5.76E-08	1.0000	0.0021	1.0043	0.0021
pu-sol-therm-022-008	1.0050	0.0001	6.79E-03	5.57E-08	1.0000	0.0023	1.0050	0.0023
pu-sol-therm-022-009	1.0038	0.0001	6.41E-03	5.42E-08	1.0000	0.0024	1.0038	0.0024
pu-sol-therm-028-001	1.0079	0.0001	1.54E-02	1.04E-07	1.0000	0.0012	1.0079	0.0012
pu-sol-therm-028-002	1.0074	0.0001	1.36E-02	9.35E-08	1.0000	0.0012	1.0074	0.0012
pu-sol-therm-028-003	1.0089	0.0001	1.18E-02	8.41E-08	1.0000	0.0012	1.0089	0.0012
pu-sol-therm-028-004	1.0088	0.0001	9.95E-03	7.51E-08	1.0000	0.0012	1.0088	0.0012
pu-sol-therm-028-005	1.0099	0.0001	9.08E-03	7.08E-08	1.0000	0.0012	1.0099	0.0012
pu-sol-therm-028-006	1.0111	0.0001	7.17E-03	6.18E-08	1.0000	0.0012	1.0111	0.0012

Benchmark	Calc. k_{eff}	Calc. σ	ANECF (MeV)	EALF (MeV)	Exp. k_{eff}	Exp. σ	k_{normal}	Total σ
pu-sol-therm-028-007	1.0080	0.0001	1.45E-02	9.57E-08	1.0000	0.0012	1.0080	0.0012
pu-sol-therm-028-008	1.0079	0.0001	1.28E-02	8.68E-08	1.0000	0.0012	1.0079	0.0012
pu-sol-therm-028-009	1.0100	0.0001	1.11E-02	7.85E-08	1.0000	0.0012	1.0100	0.0012
pu-sol-therm-032-001	0.9961	0.0001	1.27E-02	8.56E-08	1.0000	0.0019	0.9961	0.0019
pu-sol-therm-032-002	1.0013	0.0001	1.17E-02	8.10E-08	1.0000	0.0019	1.0013	0.0019
pu-sol-therm-032-003	1.0027	0.0001	1.04E-02	7.46E-08	1.0000	0.0019	1.0027	0.0019
pu-sol-therm-032-004	1.0024	0.0001	9.40E-03	6.98E-08	1.0000	0.0019	1.0024	0.0019
pu-sol-therm-032-005	1.0044	0.0001	8.45E-03	6.55E-08	1.0000	0.0019	1.0044	0.0019
pu-sol-therm-032-006	1.0048	0.0001	7.52E-03	6.13E-08	1.0000	0.0019	1.0048	0.0019
pu-sol-therm-032-007	1.0051	0.0001	7.14E-03	5.96E-08	1.0000	0.0019	1.0051	0.0019
pu-sol-therm-032-008	1.0044	0.0001	6.53E-03	5.67E-08	1.0000	0.0019	1.0044	0.0019
pu-sol-therm-032-009	1.0032	0.0001	6.10E-03	5.50E-08	1.0000	0.0019	1.0032	0.0019
pu-sol-therm-032-010	1.0052	0.0001	5.76E-03	5.36E-08	1.0000	0.0019	1.0052	0.0019
pu-sol-therm-032-011	1.0044	0.0001	5.58E-03	5.28E-08	1.0000	0.0019	1.0044	0.0019
pu-sol-therm-032-012	1.0037	0.0001	5.39E-03	5.20E-08	1.0000	0.0019	1.0037	0.0019
pu-sol-therm-032-013	1.0023	0.0001	1.01E-02	7.23E-08	1.0000	0.0019	1.0023	0.0019
pu-sol-therm-032-014	1.0019	0.0001	9.13E-03	6.78E-08	1.0000	0.0019	1.0019	0.0019
pu-sol-therm-032-015	1.0038	0.0001	8.22E-03	6.36E-08	1.0000	0.0019	1.0038	0.0019
pu-sol-therm-032-016	1.0038	0.0001	7.29E-03	5.97E-08	1.0000	0.0019	1.0038	0.0019
pu-sol-therm-032-017	1.0040	0.0001	6.93E-03	5.80E-08	1.0000	0.0019	1.0040	0.0019
pu-sol-therm-034-001	0.9996	0.0001	2.31E-02	1.43E-07	1.0000	0.0062	0.9996	0.0062
pu-sol-therm-034-002	1.0017	0.0001	2.49E-02	1.71E-07	1.0000	0.0044	1.0017	0.0044
pu-sol-therm-034-003	0.9994	0.0001	2.63E-02	1.99E-07	1.0000	0.0040	0.9994	0.0040
pu-sol-therm-034-004	1.0025	0.0001	2.75E-02	2.24E-07	1.0000	0.0039	1.0025	0.0039
pu-sol-therm-034-005	0.9999	0.0001	2.87E-02	2.50E-07	1.0000	0.0040	0.9999	0.0040
pu-sol-therm-034-006	1.0013	0.0001	2.97E-02	2.73E-07	1.0000	0.0042	1.0013	0.0042
pu-sol-therm-034-007	0.9987	0.0001	9.06E-02	1.44E-06	1.0000	0.0057	0.9987	0.0057
pu-sol-therm-034-008	0.9989	0.0001	9.18E-02	1.53E-06	1.0000	0.0055	0.9989	0.0055
pu-sol-therm-034-009	0.9980	0.0001	9.29E-02	1.62E-06	1.0000	0.0052	0.9980	0.0052
pu-sol-therm-034-010	0.9974	0.0001	9.50E-02	1.78E-06	1.0000	0.0052	0.9974	0.0052
pu-sol-therm-034-011	0.9986	0.0001	9.65E-02	1.91E-06	1.0000	0.0048	0.9986	0.0048
pu-sol-therm-034-012	0.9984	0.0001	9.84E-02	2.09E-06	1.0000	0.0042	0.9984	0.0042
pu-sol-therm-034-013	0.9969	0.0001	1.00E-01	2.26E-06	1.0000	0.0043	0.9969	0.0043
pu-sol-therm-034-014	0.9967	0.0001	1.02E-01	2.40E-06	1.0000	0.0044	0.9967	0.0044
pu-sol-therm-034-015	0.9974	0.0001	1.03E-01	2.49E-06	1.0000	0.0042	0.9974	0.0042
pu-sol-therm-038-001	1.0033	0.0002	4.75E-03	4.65E-08	1.0005	0.0015	1.0028	0.0015
pu-sol-therm-038-002	1.0036	0.0002	4.83E-03	4.68E-08	1.0005	0.0015	1.0031	0.0015
pu-sol-therm-038-003	1.0036	0.0002	3.80E-03	4.32E-08	1.0005	0.0018	1.0031	0.0018
pu-sol-therm-038-004	1.0016	0.0002	3.65E-03	4.27E-08	1.0005	0.0013	1.0011	0.0013
pu-sol-therm-038-005	1.0021	0.0002	3.74E-03	4.28E-08	1.0005	0.0013	1.0016	0.0013

4.3 Normality Testing

The benchmark critical experiment results are tested for normality using the modified Chi Square test, the Kolmogorov-Smirnov test, and the Lilliefors test. The test results are presented in Appendix 3.

The results demonstrate that the benchmark critical experiment data fails all three tests. In addition, the calculation results are plotted in a histogram. The binning structure and the expected number of observations are provided by the data used in the Chi Square test. The histogram is presented as Figure 1.

Figure 1 Histogram of Calculation Results

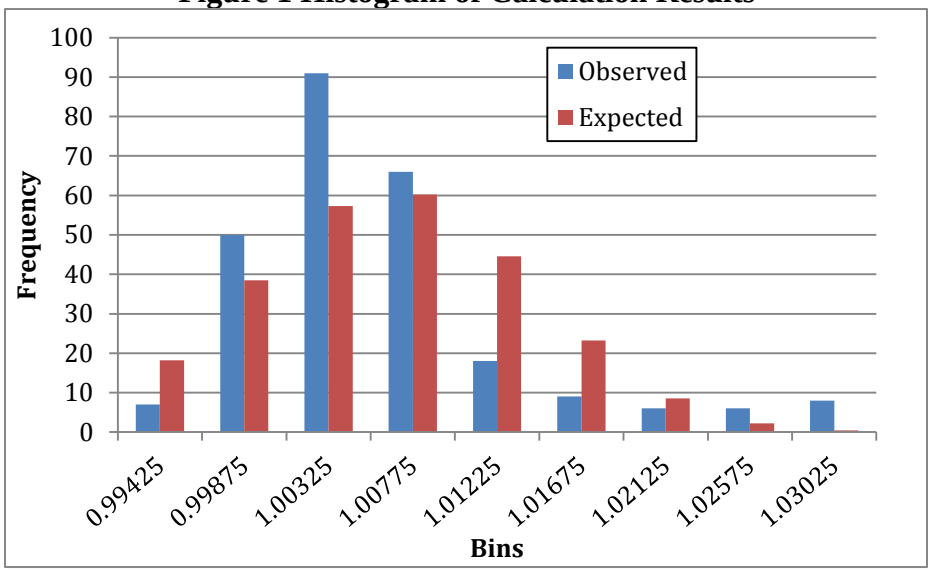

Based on the failure of the data to pass the three normality tests, and supported by visual inspection of the histogram, it is concluded that the entire benchmark critical experiment data cannot be confirmed to come from a normal distribution. Therefore, the non-parametric technique must be used to determine the USL for the entire set of validation cases.

4.4 Trend Analysis

The k_{eff} results are also analyzed to determine if any trends exists between calculated k_{eff} and important nuclear parameters. A calculational methodology should have a bias that neither has dependence on a characteristic nor is a smooth function of a parameter. If a trend exists, the bias will vary as a function of that trend over the parameter range. If no trend exists, then the bias will be constant over the area of applicability.

Three benchmark critical experiment parameters are examined: ^{240}Pu content, moderation ratio (H/^{239}Pu), and the average neutron energy causing fission (ANECF). ^{240}Pu content was examined because plutonium at LANL typically has about 2 - 4 wt% ^{240}Pu. The moderation ratio was examined because it is applicable to metal, oxide and solution. Finally ANECF was chosen to

represent the energy spectrum within the validation and because it is also indicative of the energy of the average neutron lethargy causing fission (EALF).

Graphs of the validation results for these parameters are presented as Figures 2 through 4. The graphs of the results and the trending parameters also include the coefficient of determination value (R^2) for the plotted trend line. Note, an R^2 value less than 0.3 is considered to indicate no data correlation, while an R^2 value of 0.8 or greater is indicative of data correlation; thus, a trend exist. A listing of the attempted fits to each of the three trending parameters for the complete benchmark critical experiment data set is provided in Table 4.

Table 4 Attempted Fits

Plot	Least Squares Fits	R^2
k_{normal} *vs* ^{240}*Pu wt %*	$y = 4E\text{-}05x + 1.0059$	< 0.01
x = ^{240}Pu wt%	$y = 1.0058e^{4E\text{-}05x}$	< 0.01
	$y = -2E\text{-}06x^2 + 0.0001x + 1.0056$	< 0.01
	$y = -8E\text{-}07x^3 + 4E\text{-}05x^2 - 0.0005x + 1.0074$ (see Figure 2)	0.01
k_{normal} *vs H/*^{239}*Pu*	$y = -2E\text{-}06x + 1.0072$	0.02
x = H/^{239}Pu	$y = 1.0072e^{-2E\text{-}06x}$	0.02
	$y = 3E\text{-}09x^2 - 8E\text{-}06x + 1.0082$	0.07
	$y = 2E\text{-}12x^3 - 3E\text{-}09x^2 - 4E\text{-}06x + 1.008$ (see Figure 3)	0.07
k_{normal} *vs ANECF*	$y = -0.0006x + 1.0065$	< 0.01
x = ANECF	$y = 0.0004\ln(x) + 1.0075$	0.02
	$y = 1.0065e^{-6E\text{-}04x}$	< 0.01
	$y = -0.022x^2 + 0.0366x + 1.0048$	0.32
	$y = 0.0193x^3 – 0.0769x^2 + 0.0744x + 1.0037$ (see Figure 4)	0.40
	$y = 1.0074x^{0.0004}$	0.02

Figure 2 ^{240}Pu wt% Trend Analysis

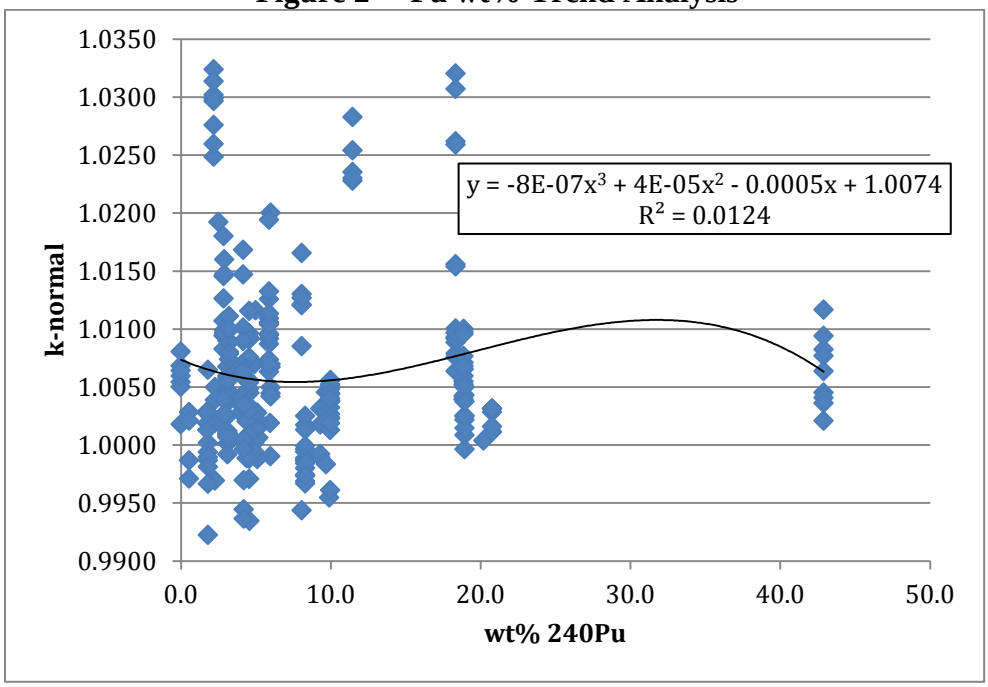

Figure 3 H/^{239}Pu Trend Analysis

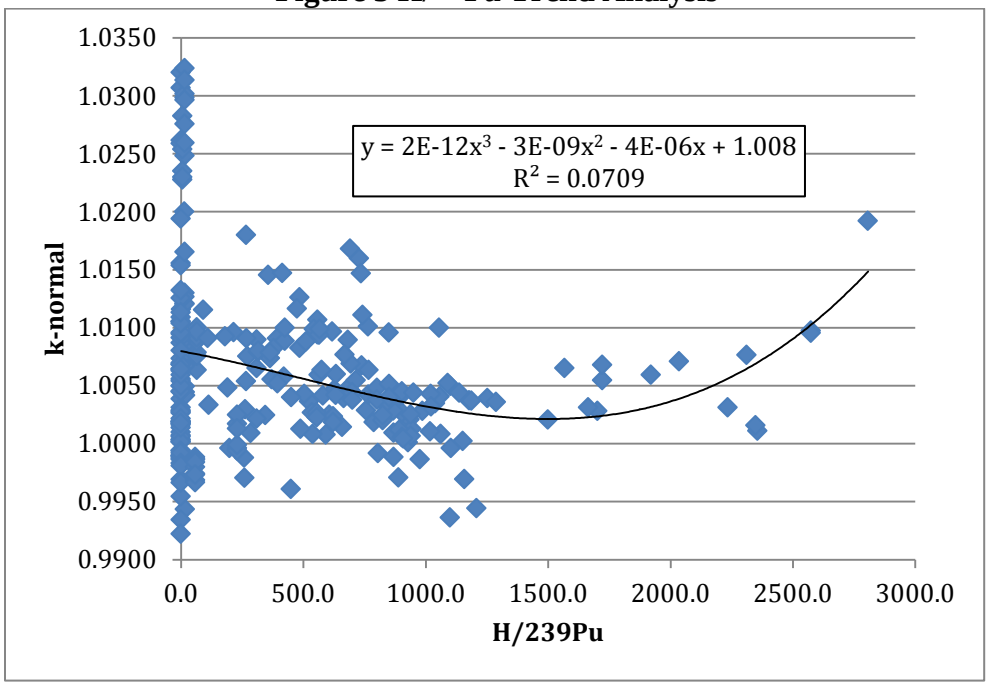

Figure 4 ANECF Trend Analysis

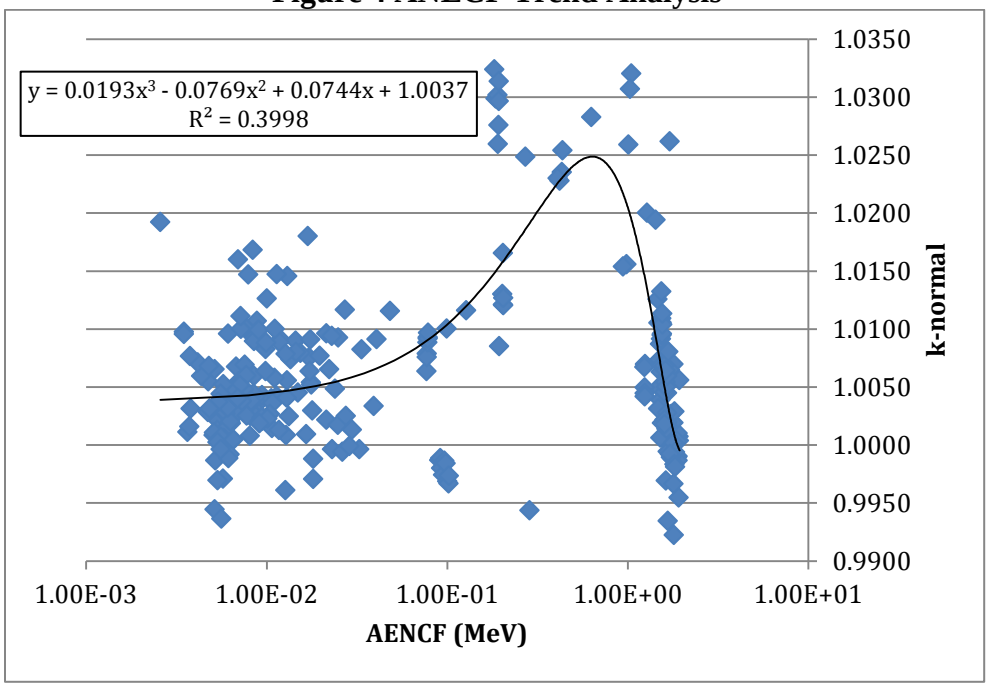

Inspection of Figures 2 through 4, and the very low calculated R^2 values, support the judgment that none of the fits presented in Table 4 adequately characterize the data distribution. Therefore, it is concluded that the data are not correlated.

Three individual data subsets, based on material form (i.e., metal, oxide, or solution), were also analyzed for potential trends in Appendix 4. The results demonstrate that no correlations exist within these individual material form subsets, either.

5.0 Area of Applicability

This validation is appropriate for plutonium systems (metal, oxide, and solution) at room temperature (293.6 K). A summary of the area of applicability derived from the entire evaluated benchmark critical experiment set is provided in Table 5. For fissile material systems or operations outside this area of applicability, an additional AoA margin may be warranted, as described in Section 3.3.

Table 5 Area of Applicability

Parameter	Area of Applicability
Fissile Material	^{239}Pu
Fissile Material Form	Pu Metal, PuO_2, and $Pu(NO_3)_4$
$H/^{239}Pu$	$0 \leq H/^{239}Pu \leq 2807$
Average Neutron Energy Causing Fission (MeV)	$0.003 \leq ANECF \leq 1.935$
^{240}Pu	0 to 42.9 wt% ^{240}Pu
Moderating Materials	none, water, graphite, polystyrene
Reflecting Materials	none, water, steel, oil, Plexiglas, polyethylene, graphite, W, Cu, U, Th, Al, Ni, Fe, Pb, Cd, Mo, Be, BeO
Other Materials	concrete, PVC, Ga, B, Gd, Ta
Geometry	cylinder array, cylinder, slab, sphere, hemisphere, stacked discs, cuboid, annular

As shown in Table 5, the area of applicability covers a wide range of material forms, moderators, reflectors, and other materials. Note that, given the similarity of polystyrene (C_8H_8) to polyethylene (CH_2 or C_2H_4), the area of applicability is judged to encompass polyethylene-moderated systems as well. Further, reflectors and other materials listed in the table may be considered equivalent when comparing to a calculational area of applicability. In terms of geometry, a reasonably wide range of shapes was evaluated. However, as stated in Section 4.0, geometrical congruence between the validation and calculations areas of applicability is not a significant concern with MCNP6.

With respect to $H/^{239}Pu$ ratio, the area of applicability covers a range between zero and 2807. Further, the figures in Section 4.4 demonstrate that the evaluated data is well distributed throughout this range, albeit more sparsely at moderation ratios greater than ~1500. With respect to ^{240}Pu content, the area of applicability covers a range between zero and 42.9 wt%. Although the figures of Section 4.4 demonstrate a large gap in the evaluated data between 27 and 43 wt%, an additional AoA margin for interpolation within this range is judged not to be necessary because the data are not correlated.

With respect to spectra, the area of applicability covers ANECFs between 0.003 and 1.935 MeV, and the figures in Section 4.4 demonstrate that the evaluated data is relatively well distributed throughout this range. Further, given the number of thermal benchmark critical experiments modeled, it is judged that the area of applicability may be extended down to ANECF values of approximately zero. ANECF was arbitrarily chosen over EALF to describe the area of applicability because there is a high degree of correlation between the two parameters (i.e., using both parameters would have been redundant).

Finally, note the following cautions which are applicable to this validation:

- Not all nuclides (stable or radioactive) of any given element are necessarily included in the validation. For example, none of the benchmark cases model deuterium; water should thus be modeled using ^{1}H only. If modeling nuclides not included in this validation additional margin or sensitivity analyses may be required.

- Only one benchmark critical experiment case includes graphite as a moderator. Modeling graphite moderation may thus require additional margin.
- With respect to neutron absorbers, multiple benchmark cases model gadolinium and cadmium. However, only one case includes boron. Modeling boron as an absorber may thus require additional margin.

If a calculation requires an extrapolation to the area of applicability, guidance may be found in LA-12683 (Reference 5), specifically Appendix E of that report. In addition, sensitivity analyses may be useful in determining if an extrapolation has a significant impact on calculated k_{eff} and in determining the magnitude of any AoA margin employed.

6.0 USL Determination

Based on the benchmark critical experiment results presented in Section 4.2, a USL is derived for the entire data set in Section 6.1, while Section 6.2 documents an evaluation justifying the derivation of a single USL.

6.1 Complete Benchmark Critical Data Set USL

Since the benchmark critical experiment results could not be shown to be normally distributed, a USL is derived using the non-parametric technique described in Section 3.4.3. For a sample size of 261, β becomes:

$$\begin{aligned} \beta &= 1 - 0.95^{n} \\ &= 1 - 0.95^{261} \\ &= 1.0000 \end{aligned}$$

From Reference 9, $\beta > 0.90$ yields a NPM of zero (because the number of sample points is sufficiently large). The USL is then calculated using the lowest calculated k_{normal} from the benchmark evaluation (PU-MET-FAST-039-001):

$$\begin{aligned} \text{USL} &= \text{Smallest } k_{normal} \text{ value in the data set} - \sigma_t - \text{NPM} - \text{MoS} - \text{AoA} \\ &= 0.9922 - 0.0022 - 0.0 - \text{MoS} - \text{AoA} \\ &= 0.9900 - \text{MoS} - \text{AoA} \end{aligned}$$

6.2 Individual Material Form Subsets

In Section 7.2 of ANSI/ANS-8.24 (Reference 10) a recommendation is made that states:

> *"The validation applicability should not be so large that a subset of the data with a high degree of similarity to the system or process would produce an upper subcritical limit that is lower than that determined for the entire set. This criterion is recommended to ensure that a subset of data that is closely related to the system or process is not nonconservatively masked by benchmarks that do not match the system as well."*

To address this recommendation, the USLs of the three individual material form subsets of the complete data set were determined and evaluated. The individual material form subsets are as follows:

- metal (based on the PU-METAL-FAST benchmarks)
- oxide (based on the PU-COMP-INTER and PU-COMP-MIXED benchmarks)
- solution (based on the PU-SOL-THERM benchmarks)

Table 6 summarizes some characteristics of these three material form data subsets, as well as the corresponding characteristics of the entire data set. Note that each individual material form subset was determined to be non-normally distributed in Appendix 3. Therefore, the subset USLs were derived using the non-parametric technique, as shown in Appendix 5. Note that the individual USLs listed in the table do not include MoS or AoA margins; they are for demonstration purposes only and are not intended for use by analysts.

Table 6 Material Form Subset Characteristics

Parameter	Metal	Oxide	Solution	All
Mean k_{eff}	1.004	1.019	1.004	1.006
Min k_{eff}	0.992	0.994	0.994	0.992
Max k_{eff}	1.020	1.032	1.019	1.032
USL*	0.990	0.978	0.988	0.990

***These USLs do not include MoS or AoA margins; these values are for demonstration purposes only and shall not be used by analysts.

From the table, the mean, minimum, and maximum normalized k_{eff} values are similar for each of the material form subsets, except that mean and maximum k_{eff} values calculated for the oxide subset are about 0.01 higher than the metal and solution subsets. This over-prediction in the oxide cases is conservative, as it will lead to a higher value of the calculated k_{eff} of the system being analyzed. The similarity in the mean and max k_{eff} in addition to the overprediction of k_{eff} in oxide cases supports a conclusion that the data does not need to be separated by material form.

Benchmark experiments were separated into material form subsets to determine if there was any correlation to nuclear parameters within the data subsets. Appendix 4 demonstrates that the material form data subsets do not individually correlate with any investigated nuclear parameter. Because there is no correlation between the material form data subsets and any of the evaluated nuclear parameters, there is no justification for separating the data by material form.

With the exception of thermal scattering from non-fissile components of a few materials, MCNP does not model the molecular structure or chemical forms of input materials. Because of this, separating the data by material form of the fissile material with no underlying correlation to nuclear parameters is untenable.

Finally, the USLs derived from the individual material form subsets are almost identical, except that the oxide USL is ~0.01 lower. However, note that the oxide USL is less than the others because it was reduced by an additional 0.01 to account for the small sample size (only 35 cases). With the reduction, the USLs range from 0.978 to 0.990 (neglecting MoS and AoA

margins). Without that statistical reduction, the three individual USLs would range from 0.988 to 0.990. Because there is such a small amount of variation in the USL when separated by material form, there is no need to separate the data.

Therefore, given the similarity in the normalized k_{eff} values (with some extra conservativism for oxides), the lack of any correlation in the individual material form subsets, the fact that MCNP does not model molecular structure, and the small spread in USLs, it is concluded herein that the overall data set is not nonconservatively masking any characteristics of the individual material form subsets. Therefore, a single USL derived from the combined data set is appropriate.

7.0 Conclusion

For the combined area of applicability defined in Section 5.0, it is concluded that the following USL may be used:

$$USL = 0.990 - MoS - AoA$$

Therefore, a k_{eff} calculated by an MCNP6 analysis is required to meet the following condition:

$$\mathbf{k_{eff} + 2\sigma \leq 0.990 - MoS - AoA}$$

where k_{eff} and σ are the calculated k_{eff} and Monte Carlo statistical uncertainty associated with the MCNP6 calculation using the ENDF/B-VII.1 continuous energy group cross section library.

As described in Section 3.2, guidance for the selection of an appropriate MoS may be found in Reference 11. As described in Section 3.3, for systems which are outside the validation area of applicability, an additional margin may be necessary. Guidance may be found in LA-12683 (Reference 5).

8.0 References

1. *International Handbook of Evaluated Criticality Safety Benchmark Experiments*, NEA/NCS/DOC (95)03, Organization for Economic Cooperation and Development, September 2012.

2. *Initial MCNP6 Release Overview - MCNP6 version 1.0*, LA-UR-13-22934, Los Alamos National Laboratory.

3. F.B. Brown, B.C. Kiedrowski, J.S. Bull, *Verification of MCNP5-1.60 and MCNP6.1 for Criticality Safety Applications*, LA-UR-13-22196, Los Alamos National Laboratory Report, 2013.

4. *Nuclear Criticality Safety in Operations with Fissionable Material Outside Reactors*, ANSI/ANS-8.1-2014, American Nuclear Society.

5. *Forecast of Criticality Benchmark Experiments and Experimental Programs Needed to Support Nuclear Operations in the United States of America: 1994-1999*, LA-12683 (Appendix E), Los Alamos, March, 1994.

6. Hollander, M., and D. A. Wolfe, *Nonparametric Statistical Methods*, John Wiley & Sons, 1973.

7. *Statistical Methods for Nuclear Material Management*, NUREG/CR-4604, PNL, December, 1988.

8. Natrella, M. G., *Experimental Statistics*, National Bureau of Standards Handbook 91, August, 1963.

9. J. C. Dean, R. W Tayloe, NUREG/CR-6698, *Guide for Validation of Nuclear Criticality Safety Calculational Methodology*, January 2001.

10. *Validation of Neutron Transport Methods for Nuclear Criticality Safety Calculations*, ANSI/ANS-8.24-2007, American Nuclear Society.

11. *Criticality Safety Evaluations*, NCS-GUIDE-01.

APPENDIX 1: BENCHMARK i/o FILES

Input and output files are stored on the NCSD common drive in the following directory:

Common/NCS Memos/TECHs/NCS-TECH-15-005/plutonium

These files were also archived on the High Performance Storage System (HPSS) as follows:

hpss/ncs-sqm/ML/NCS-TECH-15-005/plutonium.tar

hpss/ncs-sqm/ML/NCS-TECH-15-005/plutonium.tar-index.txt

APPENDIX 2: BENCHMARK EXPERIMENTS

This appendix presents brief descriptions of the benchmarks used in this validation report. Following these descriptions, data for each benchmark experiment is tabulated. Note that only the main materials utilized in the benchmark critical experiments are listed under "Other Materials" in this table. For a complete list of nuclides utilized in the benchmark critical experiments, see Table 1.

k_∞ Experiments in Intermediate Neutron Spectra for ^{239}Pu (PU-COMP-INTER-001): The experimental program comprised a series of small-sample k_∞ experiments in intermediate neutron spectra. The experiments were performed at the HECTOR (Hot Enriched Carbon-moderated Thermal Oscillator Reactor) zero-power, graphite-moderated reactor at Winfrith, United Kingdom, during the late 1960s. The plutonium elements, within the test region for the HPG (Homogeneous Plutonium Graphite) experiment, contained a mixture of plutonium powder (5% ^{240}Pu), boron and graphite.

Polystyrene-Moderated PuO_2 (PU-COMP-MIX-001 and -002): Thirty-four critical experiments involving unreflected and Plexiglas-reflected arrays of PuO_2/polystyrene cubes (compacts) are reported in Reference 1. The five unreflected experiments are evaluated in PU-COMP-MIX-001 with the 29 Plexiglas reflected experiments are evaluated in PU-COMP-MIX-002. Experimental arrays were constructed from PuO_2/polystyrene cubes with H/Pu ratios of 0.04, 5, 15, and 50.

Bare Sphere of ^{239}Pu Metal (^{239}Pu Jezebel) (PU-MET-FAST-001): In the mid-1950s, the ^{239}Pu Jezebel critical assembly was fabricated and operated at the Los Alamos Scientific Laboratory (LASL). There were three Jezebel assemblies built, one using Pu (4.5 at% ^{240}Pu) and referred to as the ^{239}Pu Jezebel, one using Pu (20 at% ^{240}Pu) and referred to as the ^{240}Pu or "dirty" Jezebel, and one using ^{233}U and referred to as the ^{233}U Jezebel. Only the ^{239}Pu Jezebel is described in this evaluation. The ^{239}Pu Jezebel was a minimally reflected δ-phase ^{239}Pu critical assembly, nearly spherical in shape.

Bare Sphere of ^{239}Pu Metal (^{240}Pu Jezebel) (PU-MET-FAST-002): As discussed above, three different Jezebel critical assemblies were built at LASL. Only the ^{240}Pu Jezebel is described in this report. The ^{240}Pu Jezebel was an unreflected, or bare, δ-phase ^{240}Pu critical assembly, nearly spherical in shape.

Unmoderated Pu Metal Button Array (PU-MET-FAST-003): Between 1965 and 1969 at the Lawrence Livermore Laboratory, plutonium metal "parts" weighing 3 kg and 6 kg were used to form reflected and unreflected arrays, of various sizes, on an aluminum table. An array was formed with half of the units on each side of a split table. A center-to-center spacing in both the vertical and lateral dimensions was chosen, and then the table was remotely pushed together.

Benchmark Critical Experiment of a Plutonium Sphere Reflected by Tungsten or Beryllium (PU-MET-FAST-005 and -018): In 1958, an experiment was performed at LASL using a slightly subcritical spherical mass of δ-phase plutonium reflected by tungsten or

beryllium. The experiment was performed using the Planet universal assembly machine. The core was composed of two hemispheres of δ-phase plutonium alloy having a diameter of 3.970 inches and plated with 0.005-inch-thick nickel with a 0.85-inch diameter source cavity in the center of the two hemispheres. Hemishells of various thicknesses were constructed to enclose the plutonium hemispheres.

Plutonium Sphere Reflected by Normal Uranium Using Flattop (PU-MET-FAST-006): In the mid-1960s a critical experiment was performed at LASL using a spherical δ-phase plutonium core reflected by normal uranium. Delayed critical was achieved. The experiment was performed using the Flattop critical assembly machine. This Flattop assembly has a core of δ-phase plutonium metal alloy, enclosed in a thick normal uranium reflector. The core is composed of two hemispheres of plutonium metal. Both halves combined to form a sphere with an outside diameter of 3.586 inches, which includes the Ni coating.

Benchmark Critical Experiment of a Thorium Reflected Plutonium Sphere (PU-MET-FAST-008): From December 1960 through November 1961, a critical assembly was operated at LASL using a spherical mass of δ-phase plutonium closely reflected by thorium. The experiment was designed to study the neutronic properties of thorium in support of a potential fast, ^{233}U breeder reactor. The average of the results for two critical experimental configurations was used to determine the final critical mass. The experiment was performed using the Thor assembly machine, a modification of the Planet universal assembly machine. The plutonium core was constructed of three major parts; an upper polar cap, a lower polar cap, and a central section. Together, the three parts approximated a sphere 10.59 cm in diameter when assembled. The upper polar cap and central section remained stationary while the lower polar cap was located on a pneumatic lift. The central section had a 1.27-cm-diameter glory hole, which was filled with plutonium as needed.

Plutonium Sphere Reflected by Aluminum (PU-METAL-FAST-009): In 1960 a critical experiment was performed at LASL using a spherical mass of δ-phase plutonium reflected by type 2014 aluminum. Measurements were taken with a single spherical mass of plutonium and three different reflector thicknesses. Measurements with the first two reflector thicknesses resulted in subcritical configurations, and measurements with the final reflector thickness yielded a slightly supercritical configuration. A curve was fitted to the three data points to derive the critical mass. The experiment was conducted using the COMET universal assembly machine. Two hemispheres with diameters of 4.34 inches were constructed of δ-phase plutonium alloy and plated with 0.005 inches of nickel. The upper hemisphere had a cylindrical central source cavity ½ inch deep and ½ inch diameter. The source cavity could accommodate either a fission source or a close fitting piece of plutonium. The nickel coated plutonium hemispheres made up the core. Nested hemishells of type 2014 aluminum were constructed to enclose the plutonium hemispheres.

Benchmark Critical Experiment of a Delta-Phase Plutonium Sphere Reflected by Normal Uranium (PU-METAL-FAST-010): In 1958, an experiment was performed at LASL using a slightly subcritical spherical mass of δ-phase plutonium reflected by normal uranium. The experiment was performed using the Planet universal assembly machine. Two hemispheres with

a 0.85-inch-diameter central source cavity and a diameter of 3.970 inches were constructed of δ-phase plutonium alloy and plated with 0.005-inch-thick nickel. Hemishells of various thicknesses of normal uranium were constructed to enclose the plutonium hemispheres.

Benchmark Critical Experiment of a Water Reflected Alpha-Phase Plutonium Sphere (PU-MET-FAST-011): In 1968, an experiment was performed at LASL using two subcritical spherical masses of α-phase plutonium reflected by water. From the two subcritical inverse multiplication measurements, an accurate prediction was made of the critical mass. The sphere was painstakingly fabricated to obtain highly pure and highly dense plutonium. The plutonium was electro-refined to produce metal with total impurities of 230 ppm and cast into two split ingots. Two hemispheres were constructed from the split ingots, and the pieces were shrink-fitted together and machined to exacting tolerances.

Uranium-Reflected Array of Plutonium Fuel Rods (PU-MET-FAST-012, -013, -014, and -015): Experiments on the critical assembly BR-1-1 were performed in 1956 - 1962 at the Institute of Physics and Power Engineering (IPPE), Obninsk, Russia. The core was a cylindrical arrangement of short, close-packed, stainless-steel-clad rods of plutonium metal (97.6 at% ^{239}Pu) reflected on all sides by thick depleted uranium (-012), copper (-013), nickel (-014), or iron (-015). The assembly was located on a steel platform with thickness 2.5 cm in the center of a cell with dimensions 12 by 6 by 6.5 m high.

Flooded 3x3x3 Arrays of 3-kg Plutonium Metal Cylinders - Phase I (PU-MET-FAST-016): In 1982, a set of critical experiments was conducted at the Rocky Flats Critical Mass Laboratory (CML). Plutonium metal cylinders were assembled into a 3x3x3 array and flooded with water. For each of the experiments, horizontal and vertical spacing were chosen and water was added until the array was critical. Twenty-seven 3-kg plutonium metal parts were used in these experiments. The plutonium part consisted of a machined right circular cylinder of plutonium metal contained in a seamless aluminum can with a mild steel lid.

Sphere of Plutonium Reflected by Beryllium or Depleted Uranium (PU-MET-FAST-019 and -020): The experiments described in these evaluations are critical configurations that were assembled in the 1980s using the VNIITF Criticality Test Facility (CTF). The assembly is a sphere of plutonium reflected by beryllium or depleted uranium, divided into two parts and separated by a gap.

Beryllium- and Beryllium Oxide-Reflected Cylinders of Plutonium (PU-MET-FAST-021): The experiments presented in this report were performed in 1987. The critical assemblies are plutonium cylinders reflected by beryllium or beryllium oxide on their ends. Two such critical assemblies have been built and are taken for the detailed description. Each critical assembly has an identical cylindrical core of 95 at% ^{239}Pu and end reflectors of Be or BeO. Each assembly consists of two almost equal parts, divided by a gap. The bottom part is movable, and the top is immovable.

Bare and Reflected Spherical Assemblies of ^{239}Pu (δ, 98%) (PU-MET-FAST-022, -023, -024, -025, -026, -035, -036, -039, and -040): Criticality measurements of bare or reflected

(graphite, polyethylene, steel, lead, cadmium/polyethylene, duralumin, or copper) δ-phase metal ^{239}Pu (98%) were carried out in the 1960s at the VNIIEF CTF. The assembly cores included five or six spherical layers of fissile material. Some cores included central cavities, and some of these were filled with additional plutonium. The reflectors consisted of one or more layers with varying outer radii. Each assembly consisted of two separate units: an upper unit and a lower (movable) unit.

Polyethylene-Reflected Spherical Assembly of ^{239}Pu (δ, 89%) (PU-MET-FAST-027 and -028): Criticality measurements of polyethylene- or steel-reflected, δ-phase metal ^{239}Pu (89%) were carried out in 1965 at the VNIIEF CTF. The assembly cores included a central cavity and five spherical layers of fissile material. The reflectors consisted of multiple layers with varying outer radii. Each assembly consisted of two separate units: an upper unit and a lower (movable) unit.

Bare and Reflected Spherical Assemblies of ^{239}Pu (α, 88%) (PU-MET-FAST-029, -030, -031, and -041): Criticality measurements of bare or reflected (graphite, polyethylene, steel, or depleted uranium) α-phase metal ^{239}Pu (88%) were carried out in 1965 at the VNIIEF CTF. The assembly cores included three to five spherical layers of fissile material (some cores included central cavities). The reflectors consisted of one or more layers with varying outer radii. Each assembly consisted of two separate units: an upper unit and a lower (movable) unit.

Plutonium Sphere Reflected by Beryllium (PU-MET-FAST-038): The BERP (BEryllium Reflected Plutonium) Ball experiments were conducted with an α-phase plutonium sphere reflected by beryllium at the Planet critical assembly at the Los Alamos Critical Experiments Facility (LACEF) in 1986. The stainless steel-clad plutonium sphere was cast and turned to a mean diameter of 7.5876 cm. Four beryllium hemispheres provide neutron reflection to the system, with a total beryllium reflector thickness of 3.349 inches.

Plutonium Hemispheres Reflected by Steel and Oil (PU-MET-FAST-042): This benchmark examines fifteen, partially oil-reflected hemispherical assemblies, representing a series of unique, steel-oil reflected experiments. Fourteen of these assemblies had close-fitting steel hemishell reflectors, used to determine the effective critical reflector height of oil with varying steel-reflector thickness. The first case represents a bare oil-reflected plutonium hemisphere. With each subsequent case, a thin steel hemishell of approximately one-third of a centimeter is added to the assembly of the previous case. The final case thus represents the original plutonium assembly in Case 1 with a series of steel hemishells with total thickness of approximately 4.67 cm. The simplified models in this benchmark critical experiment were used in the validation.

Plutonium (5.1 wt% ^{240}Pu) Metal Sphere with Beryllium, Graphite, Aluminum, Iron, and Molybdenum Tampers and Polyethylene Reflectors (PU-MET-FAST-044): Between January 1973 and September 1975, experiments involving a plutonium-alloy core with metal/graphite tampers and a polyethylene reflector were conducted at LASL. The experiments used a 9.76 kg plutonium (5.1 wt% ^{240}Pu)-alloy core, which is often referred to as the “Thor core”. This nearly spherical core consisted of three nickel-coated sections. In each experimental assembly, the plutonium-alloy core was surrounded by a close-fitting inner tamper shell and an outer

polyethylene reflector shell. The purpose of these experiments was to determine the critical polyethylene reflector thicknesses required with various tampers surrounding the plutonium-alloy core. A critical configuration was attained for three of the tamper materials (C, Fe and Al). The critical polyethylene reflector masses for configurations involving the other two tamper materials (Mo, Be) were determined by extrapolation of the approach-to-critical experiments. The benchmark critical experiments were performed using the COMET assembly machine.

Critical Experiments Performed for LAMPRE, the Los Alamos Molten Plutonium Reactor (PU-MET-FAST-045): This series of critical experiments was performed in 1957 to support construction and operation of the Los Alamos Molten Plutonium Reactor (LAMPRE), operated at LASL between May 1960 and December 1965. This set of critical experiments was known as LCX-I. The experiments were performed to 1) establish the critical mass for LAMPRE, 2) establish the effectiveness of various control schemes, and 3) determine power and flux distributions. Critical mass measurements using LCX-I were performed using three different core compositions and three different metal reflectors resulting in seven critical configurations. The LCX-I core was composed of Pu-Ni discs, Ta discs, and reduced-density Al discs placed inside of a core sleeve. The core sleeve rested on the lower reflector, which in turn rested on a cylindrical block of polyethylene on a hydraulic lift. The upper half of the assembly consisted of a water tank with a central cavity that contained the top and radial metal reflectors. The lower part of the assembly could be inserted into the upper part of the assembly to accomplish criticality or an approach-to-critical.

Water-Reflected 11.5-inch Diameter Spheres of Plutonium Nitrate Solutions (PU-SOL-THERM-001): Evaluated in this report are experiments performed at the Battelle Pacific Northwest Laboratories (PNL) Critical Mass Laboratory (CML). This benchmark consists of six experiments with a stainless steel spherical shell, 11.5 inches in diameter, surrounded by an effectively infinite water reflector. The solution was plutonium nitrate with the plutonium having 4.57 wt% ^{240}Pu.

Bare and Water-Reflected Spheres of Plutonium Nitrate Solutions (PU-SOL-THERM-002, -003, -004, -005, -006, -007, and -011): Experiments performed in the P-11 area of the Hanford Reservation in the early 1950s are evaluated in this report. The experiments were directed toward determining the effect of geometry, concentration, foreign atoms, plutonium isotopic content, neutron reflection, and temperature on the critical mass of light water moderated and reflected homogeneous plutonium solutions. The plutonium nitrate solution was contained in nominally 12-, 13-, 14-, 15-, 16-, or 18-inch diameter spheres, which were inside a large cylindrical tank that provided effectively full water reflection around the sphere. The 11.5-inch experiments involved a partially filled sphere, while the other spheres were completely full.

Unreflected 48-inch-Diameter Sphere of Plutonium Nitrate Solution (PU-SOL-THERM-009): Evaluated in this report are three experiments performed at the PNL CML in a 48-inch-diameter bare sphere. Minimum critical plutonium concentrations were determined for ^{239}Pu-nitrate solutions, by using the data from the 48-inch sphere experiments and from eight experiments in smaller spheres.

Water-Reflected 9-, 10-, 11-, and 12-inch-Diameter Cylinders of Plutonium Nitrate Solutions (PU-SOL-THERM-010): Thirty-five critical experiments with cylindrical reactors were performed in the P-11 area of the Hanford Reservation in the early 1950s. The P-11 series of experiments were directed toward determining the effect of geometry, concentration, foreign atoms, plutonium isotopic content, neutron reflection, and temperature on the critical mass of light water moderated and reflected homogeneous plutonium solutions. The plutonium nitrate solutions were contained in a series of cylinders with inside diameters of 9, 10, 11, and 12 inches. The cylindrical reactors were inside a large cylindrical water-filled tank that provided at least 12 inches of water reflection around the cylinders in all directions. Each cylinder was fitted with a movable water-filled piston 'tamper' (top reflector) which was 12 inches thick.

Criticality of Plutonium Nitrate Solution in a Large Water-Reflected Cubic Tank (130 x 130 x 100 cm) (19% ^{240}Pu) (PU-SOL-THERM-012): The experimental program considered plutonium nitrate solution in a large right parallelepiped tank. The tank was either fully reflected by water on six sides, water reflected on five sides, or not water reflected. A plutonium concentration range of 13.2 to 105 g/l was examined. The plutonium contained 18.88% ^{240}Pu. These experiments, performed at the VALDUC facility (CEA-FRANCE) in 1974, were subcritical approaches extrapolated to critical. The multiplication factor reached was very close to 1.000 (within 0.1%). Five fully water-reflected experiments and eight experiments water-reflected on five sides are evaluated.

Water-Reflected 24-inch Diameter Cylinder Of Plutonium Nitrate Solution (PU-SOL-THERM-018): In 1971, experiments involving water-reflected cylinders of plutonium nitrate solutions from high burn-up fuel (~42.9 wt% ^{240}Pu) were performed at the PNL CML. The purpose of the experiments was to “establish the combined effects of the various isotopes of plutonium on criticality.” There were nine reported configurations corresponding to plutonium concentration in the solution varying from ~40 to ~140 g Pu/liter. Critical heights (and volumes) were determined for each plutonium concentration.

Plutonium Nitrate Solution in a Water-Reflected Annular Cylinder Tank (PU-SOL-THERM-022, -028, and -032): The experimental program considered plutonium nitrate solution in an annular cylinder tank. The outer and inner diameters of the tank were 50 cm/20 cm or 50 cm/30 cm. The tank was reflected by water on the side and at the bottom. A plutonium concentration range of 28.5 to 165 g/l was examined. The plutonium contained 3.22 or 18.88% ^{240}Pu. These experiments, performed at the Valduc facility (CEA-FRANCE) in the 19060s and 1970s, were subcritical approaches extrapolated to critical. The multiplication factor reached was very close to 1.000 (within 0.1%).

Plutonium (8.3 wt% ^{240}Pu) Nitrate Solution with Gadolinium in Water-Reflected 24-inch Diameter Cylinder (PU-SOL-THERM-034): Between September 1970 and March 1971, experiments involving water-reflected cylinders (24-inch diameter) of plutonium nitrate solutions poisoned with gadolinium nitrate were performed at the PNL CML. The purpose of the experiments was to “establish the effect of a soluble neutron absorber on the criticality of plutonium nitrate solutions.” There are fifteen reported configurations at a plutonium concentration of either 116 or 363 g Pu/liter. The plutonium contained 8.3 wt% ^{240}Pu. Critical

heights and volumes were determined at gadolinium concentrations varying from 0 to 20.25 g Gd/liter for the fifteen configurations.

Plutonium Temperature Effect Program - Low Concentrated (20, 15 Or 14.3 g/L) Plutonium Nitrate Solutions at Room Temperature (PU-SOL-THERM-038): The main goal of the French Plutonium Temperature Effect Experimental Program is to effectively show that a positive temperature effect exists for diluted plutonium solutions. The experiments were conducted in the "Apparatus B" facility at the CEA VALDUC research center in France and involved 17 sub-critical approaches using plutonium nitrate solutions with concentrations of 14.3, 15, and 20 g/l at temperatures ranging from 22 - 40°C. The experiments started in late 2006 and were concluded in July 2007. The experimental set-up consists of two concentric cylindrical vessels: an inner vessel which accommodates the plutonium solutions during the experiment and an outer vessel which provides neutron reflection by a water layer laterally and under the plutonium vessel.

Table 7 Benchmark Critical Experiment Summary

Benchmark	^{240}Pu wt%	Form	Geometry	Moderator / Reflector	H/^{239}Pu	Other Materials
pu-comp-inter-001-001	5.0	PuO2	Infinite	Graphite/None	0.4	B
pu-comp-mixed-001-001	18.4	PuO2	Slab	Water/None	0.1	Concrete
pu-comp-mixed-001-002	11.5	PuO2	Slab	Polystyrene/None	5.9	Concrete
pu-comp-mixed-001-003	2.2	PuO2	Slab	Polystyrene/None	15.5	Concrete
pu-comp-mixed-001-004	8.1	PuO2	Slab	Polystyrene/None	16.4	Concrete
pu-comp-mixed-001-005	18.4	PuO2	Slab	Polystyrene/None	65.4	Concrete
pu-comp-mixed-002-001	18.4	PuO2	Slab	Polystyrene/Plexiglas	0.1	None
pu-comp-mixed-002-002	18.4	PuO2	Slab	Polystyrene/Plexiglas	0.1	None
pu-comp-mixed-002-003	18.4	PuO2	Slab	Polystyrene/Plexiglas	0.1	None
pu-comp-mixed-002-004	18.4	PuO2	Slab	Polystyrene/Plexiglas	0.1	None
pu-comp-mixed-002-005	18.4	PuO2	Slab	Polystyrene/Plexiglas	0.1	None
pu-comp-mixed-002-006	11.5	PuO2	Slab	Polystyrene/Plexiglas	5.9	None
pu-comp-mixed-002-007	11.5	PuO2	Slab	Polystyrene/Plexiglas	5.9	None
pu-comp-mixed-002-008	11.5	PuO2	Slab	Polystyrene/Plexiglas	5.9	None
pu-comp-mixed-002-009	11.5	PuO2	Slab	Polystyrene/Plexiglas	5.9	None
pu-comp-mixed-002-010	2.2	PuO2	Slab	Polystyrene/Plexiglas	15.5	None
pu-comp-mixed-002-011	2.2	PuO2	Slab	Polystyrene/Plexiglas	15.5	None
pu-comp-mixed-002-012	2.2	PuO2	Slab	Polystyrene/Plexiglas	15.5	None
pu-comp-mixed-002-013	2.2	PuO2	Slab	Polystyrene/Plexiglas	15.5	None
pu-comp-mixed-002-014	2.2	PuO2	Slab	Polystyrene/Plexiglas	15.5	None
pu-comp-mixed-002-015	2.2	PuO2	Slab	Polystyrene/Plexiglas	15.5	None
pu-comp-mixed-002-016	2.2	PuO2	Slab	Polystyrene/Plexiglas	15.5	None
pu-comp-mixed-002-017	8.1	PuO2	Slab	Polystyrene/Plexiglas	15.5	None
pu-comp-mixed-002-018	8.1	PuO2	Slab	Polystyrene/Plexiglas	15.5	None
pu-comp-mixed-002-019	8.1	PuO2	Slab	Polystyrene/Plexiglas	15.5	None
pu-comp-mixed-002-020	8.1	PuO2	Slab	Polystyrene/Plexiglas	15.5	None
pu-comp-mixed-002-021	8.1	PuO2	Slab	Polystyrene/Plexiglas	15.5	None
pu-comp-mixed-002-022	8.1	PuO2	Slab	Polystyrene/Plexiglas	15.5	None
pu-comp-mixed-002-023	18.4	PuO2	Slab	Polystyrene/Plexiglas	65.4	None
pu-comp-mixed-002-024	18.4	PuO2	Slab	Polystyrene/Plexiglas	65.4	None
pu-comp-mixed-002-025	18.4	PuO2	Slab	Polystyrene/Plexiglas	65.4	None
pu-comp-mixed-002-026	18.4	PuO2	Slab	Polystyrene/Plexiglas	65.4	None
pu-comp-mixed-002-027	18.4	PuO2	Slab	Polystyrene/Plexiglas	65.4	None
pu-comp-mixed-002-028	18.4	PuO2	Slab	Polystyrene/Plexiglas	65.4	None
pu-comp-mixed-002-029	18.4	PuO2	Slab	Polystyrene/Plexiglas	65.4	None
pu-met-fast-001-001	4.5	Metal	Sphere	None	0.0	Ga
pu-met-fast-002-001	20.2	Metal	Sphere	None	0.0	Ga
pu-met-fast-003-103	6.0	Metal	Cylinder Array	None/Polyethylene	0.0	Al, Steel

Benchmark	^{240}Pu wt%	Form	Geometry	Moderator / Reflector	H/^{239}Pu	Other Materials
pu-met-fast-005-001	4.9	Metal	Sphere	None/W	0.0	Ga, Ni
pu-met-fast-006-001	4.8	Metal	Sphere	None/U	0.0	Ga
pu-met-fast-008-001	5.1	Metal	Sphere	None/Th	0.0	Ga
pu-met-fast-009-001	4.9	Metal	Sphere	None/Al	0.0	Ga
pu-met-fast-010-001	4.9	Metal	Sphere	None/U	0.0	Ga
pu-met-fast-011-001	5.2	Metal	Sphere	None/Water	0.0	None
pu-met-fast-012-001	2.3	Metal	Cylinder	None/U	0.0	Ga, Cu, Steel
pu-met-fast-013-001	2.3	Metal	Cylinder	None/Cu	0.0	Ga, Cu, Steel
pu-met-fast-014-001	2.3	Metal	Cylinder	None/Ni	0.0	Ga, Cu, Steel
pu-met-fast-015-001	2.3	Metal	Cylinder	None/Fe	0.0	Ga, Cu, Steel
pu-met-fast-016-001	6.0	Metal	Cylinder Array	Water/Water	14.2	Al, Steel
pu-met-fast-016-002	6.0	Metal	Cylinder Array	Water/Water	16.3	Al, Steel
pu-met-fast-016-003	6.0	Metal	Cylinder Array	Water/Water	16.9	Al, Steel
pu-met-fast-016-004	6.0	Metal	Cylinder Array	Water/Water	17.2	Al, Steel
pu-met-fast-016-005	6.0	Metal	Cylinder Array	Water/Water	17.3	Al, Steel
pu-met-fast-016-006	6.0	Metal	Cylinder Array	Water/Water	17.1	Al, Steel
pu-met-fast-018-001	4.9	Metal	Sphere	None/Be	0.0	Ga
pu-met-fast-019-001	9.3	Metal	Sphere	None/Be	0.0	Ga, Cu, Steel
pu-met-fast-020-001	9.3	Metal	Sphere	None/U	0.0	Al, Ga, Fe
pu-met-fast-021-001	4.6	Metal	Stacked Discs	None/Be	0.0	Al, Steel
pu-met-fast-021-002	4.6	Metal	Stacked Discs	None/BeO	0.0	Al, Steel
pu-met-fast-022-001	1.8	Metal	Sphere	None	0.0	Ga
pu-met-fast-023-001	1.8	Metal	Sphere	None/Graphite	0.0	Ga
pu-met-fast-024-001	1.8	Metal	Sphere	None/Polyethylene	0.0	Ga
pu-met-fast-025-001	1.8	Metal	Sphere	None/Steel	0.0	Ga
pu-met-fast-026-001	1.8	Metal	Sphere	None/Steel	0.0	Ga
pu-met-fast-027-001	9.3	Metal	Sphere	None/Polyethylene	0.0	Ga
pu-met-fast-028-001	9.3	Metal	Sphere	None/Steel	0.0	Ga
pu-met-fast-029-001	9.9	Metal	Sphere	None	0.0	None
pu-met-fast-030-001	9.7	Metal	Sphere	None/Graphite	0.0	None
pu-met-fast-031-001	9.7	Metal	Sphere	None/Polyethylene	0.0	None
pu-met-fast-032-001	9.7	Metal	Sphere	None/Steel	0.0	None
pu-met-fast-035-001	1.8	Metal	Sphere	None/Pb	0.0	Ga
pu-met-fast-036-001	1.8	Metal	Sphere	None/Polyethylene & Cd	0.0	Ga
pu-met-fast-038-001	6.0	Metal	Sphere	None/Be	0.0	Ga, Al, Steel
pu-met-fast-039-001	1.8	Metal	Sphere	None/Al	0.0	Ga, Ni
pu-met-fast-040-001	1.8	Metal	Sphere	None/Cu	0.0	Ga, Ni
pu-met-fast-041-001	10.0	Metal	Sphere	None/U	0.0	None
pu-met-fast-042-001	5.9	Metal	Hemisphere	None/Oil	0.1	Steel
pu-met-fast-042-002	5.9	Metal	Hemisphere	None/Oil	0.1	Steel
pu-met-fast-042-003	5.9	Metal	Hemisphere	None/Oil	0.1	Steel
pu-met-fast-042-004	5.9	Metal	Hemisphere	None/Oil	0.1	Steel
pu-met-fast-042-005	5.9	Metal	Hemisphere	None/Oil	0.1	Steel
pu-met-fast-042-006	5.9	Metal	Hemisphere	None/Oil	0.1	Steel
pu-met-fast-042-007	5.9	Metal	Hemisphere	None/Oil	0.1	Steel
pu-met-fast-042-008	5.9	Metal	Hemisphere	None/Oil	0.1	Steel
pu-met-fast-042-009	5.9	Metal	Hemisphere	None/Oil	0.1	Steel
pu-met-fast-042-010	5.9	Metal	Hemisphere	None/Oil	0.1	Steel
pu-met-fast-042-011	5.9	Metal	Hemisphere	None/Oil	0.1	Steel
pu-met-fast-042-012	5.9	Metal	Hemisphere	None/Oil	0.1	Steel
pu-met-fast-042-013	5.9	Metal	Hemisphere	None/Oil	0.1	Steel
pu-met-fast-042-014	5.9	Metal	Hemisphere	None/Oil	0.1	Steel
pu-met-fast-042-015	5.9	Metal	Hemisphere	None/Oil	0.1	Steel
pu-met-fast-044-001	5.1	Metal	Sphere	None/Polyethylene & Mo	0.0	Ga, Ni
pu-met-fast-044-002	5.1	Metal	Sphere	None/Polyethylene & Fe	0.0	Ga, Ni
pu-met-fast-044-003	5.1	Metal	Sphere	None/Polyethylene & Be	0.0	Ga, Ni
pu-met-fast-044-004	5.1	Metal	Sphere	None/Polyethylene & Al	0.0	Ga, Ni
pu-met-fast-044-005	5.1	Metal	Sphere	None/Polyethylene & Graphite	0.0	Ga, Ni
pu-met-fast-045-001	0.0	Metal	Stacked Discs	None/Ni	0.0	Ta, Al, Fe, Water, Poly
pu-met-fast-045-002	0.0	Metal	Stacked Discs	None/Ni & Fe	0.0	Ta, Al, Water, Poly
pu-met-fast-045-003	0.0	Metal	Stacked Discs	None/Ni & Fe	0.0	Ta, Al, Water, Poly
pu-met-fast-045-004	0.0	Metal	Stacked Discs	None/Ni	0.0	Ta, Al, Fe, Water, Poly

Benchmark	^{240}Pu wt%	Form	Geometry	Moderator / Reflector	H/^{239}Pu	Other Materials
pu-met-fast-045-005	0.0	Metal	Stacked Discs	None/Ni	0.0	Ta, Al, Fe, Water, Poly
pu-met-fast-045-006	0.0	Metal	Stacked Discs	None/Fe	0.0	Ta, Al, Ni, Water, Poly
pu-met-fast-045-007	0.0	Metal	Stacked Discs	None/Fe	0.0	Ta, Al, Ni, Water, Poly
pu-sol-therm-001-001	4.6	Pu(NO3)4	Sphere	Water/Water	371.4	Steel
pu-sol-therm-001-002	4.6	Pu(NO3)4	Sphere	Water/Water	271.5	Steel
pu-sol-therm-001-003	4.6	Pu(NO3)4	Sphere	Water/Water	215.9	Steel
pu-sol-therm-001-004	4.6	Pu(NO3)4	Sphere	Water/Water	190.4	Steel
pu-sol-therm-001-005	4.6	Pu(NO3)4	Sphere	Water/Water	180.2	Steel
pu-sol-therm-001-006	4.6	Pu(NO3)4	Sphere	Water/Water	91.2	Steel
pu-sol-therm-002-001	3.1	Pu(NO3)4	Sphere	Water/Water	524.3	Steel
pu-sol-therm-002-002	3.1	Pu(NO3)4	Sphere	Water/Water	504.9	Steel
pu-sol-therm-002-003	3.1	Pu(NO3)4	Sphere	Water/Water	451.3	Steel
pu-sol-therm-002-004	3.1	Pu(NO3)4	Sphere	Water/Water	420.5	Steel
pu-sol-therm-002-005	3.1	Pu(NO3)4	Sphere	Water/Water	392.8	Steel
pu-sol-therm-002-006	3.1	Pu(NO3)4	Sphere	Water/Water	344.2	Steel
pu-sol-therm-002-007	3.1	Pu(NO3)4	Sphere	Water/Water	308.9	Steel
pu-sol-therm-003-001	1.8	Pu(NO3)4	Sphere	Water/Water	788.0	Steel
pu-sol-therm-003-002	1.8	Pu(NO3)4	Sphere	Water/Water	756.0	Steel
pu-sol-therm-003-003	3.1	Pu(NO3)4	Sphere	Water/Water	698.9	Steel
pu-sol-therm-003-004	3.1	Pu(NO3)4	Sphere	Water/Water	681.7	Steel
pu-sol-therm-003-005	3.1	Pu(NO3)4	Sphere	Water/Water	626.6	Steel
pu-sol-therm-003-006	3.1	Pu(NO3)4	Sphere	Water/Water	562.8	Steel
pu-sol-therm-003-007	3.1	Pu(NO3)4	Sphere	Water/Water	737.8	Al
pu-sol-therm-003-008	3.1	Pu(NO3)4	Sphere	Water/Water	714.3	Al
pu-sol-therm-004-001	0.5	Pu(NO3)4	Sphere	Water/Water	987.0	Steel
pu-sol-therm-004-002	0.5	Pu(NO3)4	Sphere	Water/Water	976.9	Steel
pu-sol-therm-004-003	0.5	Pu(NO3)4	Sphere	Water/Water	934.6	Steel
pu-sol-therm-004-004	0.5	Pu(NO3)4	Sphere	Water/Water	888.9	Steel
pu-sol-therm-004-005	1.8	Pu(NO3)4	Sphere	Water/Water	942.0	Steel
pu-sol-therm-004-006	3.1	Pu(NO3)4	Sphere	Water/Water	927.4	Steel
pu-sol-therm-004-007	3.1	Pu(NO3)4	Sphere	Water/Water	891.7	Steel
pu-sol-therm-004-008	3.1	Pu(NO3)4	Sphere	Water/Water	869.0	Steel
pu-sol-therm-004-009	3.1	Pu(NO3)4	Sphere	Water/Water	805.2	Steel
pu-sol-therm-004-010	3.1	Pu(NO3)4	Sphere	Water/Water	689.4	Steel
pu-sol-therm-004-011	3.1	Pu(NO3)4	Sphere	Water/Water	592.4	Steel
pu-sol-therm-004-012	3.1	Pu(NO3)4	Sphere	Water/Water	892.7	Steel
pu-sol-therm-004-013	3.4	Pu(NO3)4	Sphere	Water/Water	903.1	Steel
pu-sol-therm-005-001	4.1	Pu(NO3)4	Sphere	Water/Water	902.8	Steel
pu-sol-therm-005-002	4.1	Pu(NO3)4	Sphere	Water/Water	867.7	Steel
pu-sol-therm-005-003	4.1	Pu(NO3)4	Sphere	Water/Water	834.4	Steel
pu-sol-therm-005-004	4.1	Pu(NO3)4	Sphere	Water/Water	765.2	Steel
pu-sol-therm-005-005	4.1	Pu(NO3)4	Sphere	Water/Water	694.1	Steel
pu-sol-therm-005-006	4.1	Pu(NO3)4	Sphere	Water/Water	633.4	Steel
pu-sol-therm-005-007	4.1	Pu(NO3)4	Sphere	Water/Water	580.6	Steel
pu-sol-therm-005-008	4.4	Pu(NO3)4	Sphere	Water/Water	868.7	Steel
pu-sol-therm-005-009	4.4	Pu(NO3)4	Sphere	Water/Water	825.1	Steel
pu-sol-therm-006-001	3.1	Pu(NO3)4	Sphere	Water/Water	1061.1	Steel
pu-sol-therm-006-002	3.1	Pu(NO3)4	Sphere	Water/Water	1017.8	Steel
pu-sol-therm-006-003	3.1	Pu(NO3)4	Sphere	Water/Water	940.1	Steel
pu-sol-therm-007-002	4.6	Pu(NO3)4	Sphere	Water/Water	109.6	Steel
pu-sol-therm-007-003	4.6	Pu(NO3)4	Sphere	Water/Water	114.0	Steel
pu-sol-therm-007-005	4.6	Pu(NO3)4	Sphere	Water/Water	267.5	Steel
pu-sol-therm-007-006	4.6	Pu(NO3)4	Sphere	Water/Water	262.0	Steel
pu-sol-therm-007-007	4.6	Pu(NO3)4	Sphere	Water/Water	265.7	Steel
pu-sol-therm-007-008	4.6	Pu(NO3)4	Sphere	Water/Water	258.5	Steel
pu-sol-therm-007-009	4.6	Pu(NO3)4	Sphere	Water/Water	259.7	Steel
pu-sol-therm-007-010	4.6	Pu(NO3)4	Sphere	Water/Water	285.0	Steel
pu-sol-therm-009-003	2.5	Pu(NO3)4	Sphere	Water/None	2806.8	Al
pu-sol-therm-010-001	2.9	Pu(NO3)4	Cylinder	Water/Water	266.9	Steel
pu-sol-therm-010-002	2.9	Pu(NO3)4	Cylinder	Water/Water	356.9	Steel
pu-sol-therm-010-003	2.9	Pu(NO3)4	Cylinder	Water/Water	484.2	Steel
pu-sol-therm-010-004	2.9	Pu(NO3)4	Cylinder	Water/Water	485.0	Steel

Benchmark	^{240}Pu wt%	Form	Geometry	Moderator / Reflector	H/^{239}Pu	Other Materials
pu-sol-therm-010-005	2.9	Pu(NO3)4	Cylinder	Water/Water	558.1	Steel
pu-sol-therm-010-006	2.9	Pu(NO3)4	Cylinder	Water/Water	558.1	Steel
pu-sol-therm-010-007	2.9	Pu(NO3)4	Cylinder	Water/Water	605.9	Steel
pu-sol-therm-010-008	2.9	Pu(NO3)4	Cylinder	Water/Water	665.4	Steel
pu-sol-therm-010-009	2.9	Pu(NO3)4	Cylinder	Water/Water	414.3	Steel
pu-sol-therm-010-010	2.9	Pu(NO3)4	Cylinder	Water/Water	535.2	Steel
pu-sol-therm-010-011	2.9	Pu(NO3)4	Cylinder	Water/Water	543.4	Steel
pu-sol-therm-010-012	2.9	Pu(NO3)4	Cylinder	Water/Water	618.3	Steel
pu-sol-therm-010-013	2.9	Pu(NO3)4	Cylinder	Water/Water	728.1	Steel
pu-sol-therm-010-014	2.9	Pu(NO3)4	Cylinder	Water/Water	849.7	Steel
pu-sol-therm-011-161	4.2	Pu(NO3)4	Sphere	Water/None	764.8	Steel
pu-sol-therm-011-162	4.2	Pu(NO3)4	Sphere	Water/None	736.0	Steel
pu-sol-therm-011-163	4.2	Pu(NO3)4	Sphere	Water/None	691.5	Steel
pu-sol-therm-011-164	4.2	Pu(NO3)4	Sphere	Water/None	681.7	Steel
pu-sol-therm-011-165	4.2	Pu(NO3)4	Sphere	Water/None	574.5	Steel
pu-sol-therm-011-181	4.2	Pu(NO3)4	Sphere	Water/None	1207.8	Steel, Cd
pu-sol-therm-011-182	4.2	Pu(NO3)4	Sphere	Water/None	1151.4	Steel, Cd
pu-sol-therm-011-183	4.2	Pu(NO3)4	Sphere	Water/None	1158.2	Steel, Cd
pu-sol-therm-011-184	4.2	Pu(NO3)4	Sphere	Water/None	1099.7	Steel, Cd
pu-sol-therm-011-185	4.2	Pu(NO3)4	Sphere	Water/None	1038.9	Steel, Cd
pu-sol-therm-011-186	4.2	Pu(NO3)4	Sphere	Water/None	908.4	Steel, Cd
pu-sol-therm-011-187	4.2	Pu(NO3)4	Sphere	Water/None	1102.6	Steel, Cd
pu-sol-therm-012-001	18.9	Pu(NO3)4	Cuboid	Water/Water	1721.6	Steel, PVC
pu-sol-therm-012-002	18.9	Pu(NO3)4	Cuboid	Water/Water	1920.1	Steel, PVC
pu-sol-therm-012-003	18.9	Pu(NO3)4	Cuboid	Water/Water	2035.4	Steel, PVC
pu-sol-therm-012-004	18.9	Pu(NO3)4	Cuboid	Water/Water	2311.6	Steel, PVC
pu-sol-therm-012-005	18.9	Pu(NO3)4	Cuboid	Water/Water	2573.3	Steel, PVC
pu-sol-therm-012-006	18.9	Pu(NO3)4	Cuboid	Water/Water	309.1	Steel, PVC
pu-sol-therm-012-007	18.9	Pu(NO3)4	Cuboid	Water/Water	393.8	Steel, PVC
pu-sol-therm-012-008	18.9	Pu(NO3)4	Cuboid	Water/Water	632.5	Steel, PVC
pu-sol-therm-012-009	18.9	Pu(NO3)4	Cuboid	Water/Water	1054.1	Steel, PVC
pu-sol-therm-012-010	18.9	Pu(NO3)4	Cuboid	Water/Water	1251.8	Steel, PVC
pu-sol-therm-012-011	18.9	Pu(NO3)4	Cuboid	Water/Water	1566.7	Steel, PVC
pu-sol-therm-012-012	18.9	Pu(NO3)4	Cuboid	Water/Water	1721.6	Steel, PVC
pu-sol-therm-012-013	18.9	Pu(NO3)4	Cuboid	Water/Water	2573.3	Steel, PVC
pu-sol-therm-018-001	42.9	Pu(NO3)4	Cylinder	Water/Water	378.8	Steel
pu-sol-therm-018-002	42.9	Pu(NO3)4	Cylinder	Water/Water	473.7	Steel
pu-sol-therm-018-003	42.9	Pu(NO3)4	Cylinder	Water/Water	564.8	Steel
pu-sol-therm-018-004	42.9	Pu(NO3)4	Cylinder	Water/Water	669.1	Steel
pu-sol-therm-018-005	42.9	Pu(NO3)4	Cylinder	Water/Water	767.4	Steel
pu-sol-therm-018-006	42.9	Pu(NO3)4	Cylinder	Water/Water	902.9	Steel
pu-sol-therm-018-007	42.9	Pu(NO3)4	Cylinder	Water/Water	1057.1	Steel
pu-sol-therm-018-008	42.9	Pu(NO3)4	Cylinder	Water/Water	1288.0	Steel
pu-sol-therm-018-009	42.9	Pu(NO3)4	Cylinder	Water/Water	1499.1	Steel
pu-sol-therm-022-001	18.9	Pu(NO3)4	Annular	Water/Water	198.5	Steel
pu-sol-therm-022-002	18.9	Pu(NO3)4	Annular	Water/Water	309.6	Steel
pu-sol-therm-022-003	18.9	Pu(NO3)4	Annular	Water/Water	538.4	Steel
pu-sol-therm-022-004	18.9	Pu(NO3)4	Annular	Water/Water	658.1	Steel
pu-sol-therm-022-005	18.9	Pu(NO3)4	Annular	Water/Water	824.9	Steel
pu-sol-therm-022-006	18.9	Pu(NO3)4	Annular	Water/Water	937.9	Steel
pu-sol-therm-022-007	18.9	Pu(NO3)4	Annular	Water/Water	1021.1	Steel
pu-sol-therm-022-008	18.9	Pu(NO3)4	Annular	Water/Water	1100.8	Steel
pu-sol-therm-022-009	18.9	Pu(NO3)4	Annular	Water/Water	1178.0	Steel
pu-sol-therm-028-001	3.2	Pu(NO3)4	Annular	Water/Water	316.2	Steel
pu-sol-therm-028-002	3.2	Pu(NO3)4	Annular	Water/Water	363.8	Steel
pu-sol-therm-028-003	3.2	Pu(NO3)4	Annular	Water/Water	424.9	Steel
pu-sol-therm-028-004	3.2	Pu(NO3)4	Annular	Water/Water	511.2	Steel
pu-sol-therm-028-005	3.2	Pu(NO3)4	Annular	Water/Water	567.4	Steel
pu-sol-therm-028-006	3.2	Pu(NO3)4	Annular	Water/Water	742.8	Steel
pu-sol-therm-028-007	3.2	Pu(NO3)4	Annular	Water/Water	316.2	Steel
pu-sol-therm-028-008	3.2	Pu(NO3)4	Annular	Water/Water	363.8	Steel
pu-sol-therm-028-009	3.2	Pu(NO3)4	Annular	Water/Water	424.9	Steel

Benchmark	^{240}Pu wt%	Form	Geometry	Moderator / Reflector	H/^{239}Pu	Other Materials
pu-sol-therm-032-001	10.0	Pu(NO3)4	Annular	Water/Water	449.5	Steel
pu-sol-therm-032-002	10.0	Pu(NO3)4	Annular	Water/Water	488.2	Steel
pu-sol-therm-032-003	10.0	Pu(NO3)4	Annular	Water/Water	555.3	Steel
pu-sol-therm-032-004	10.0	Pu(NO3)4	Annular	Water/Water	622.5	Steel
pu-sol-therm-032-005	10.0	Pu(NO3)4	Annular	Water/Water	700.7	Steel
pu-sol-therm-032-006	10.0	Pu(NO3)4	Annular	Water/Water	800.5	Steel
pu-sol-therm-032-007	10.0	Pu(NO3)4	Annular	Water/Water	850.5	Steel
pu-sol-therm-032-008	10.0	Pu(NO3)4	Annular	Water/Water	949.6	Steel
pu-sol-therm-032-009	10.0	Pu(NO3)4	Annular	Water/Water	1021.5	Steel
pu-sol-therm-032-010	10.0	Pu(NO3)4	Annular	Water/Water	1090.5	Steel
pu-sol-therm-032-011	10.0	Pu(NO3)4	Annular	Water/Water	1136.5	Steel
pu-sol-therm-032-012	10.0	Pu(NO3)4	Annular	Water/Water	1186.4	Steel
pu-sol-therm-032-013	10.0	Pu(NO3)4	Annular	Water/Water	555.3	Steel
pu-sol-therm-032-014	10.0	Pu(NO3)4	Annular	Water/Water	622.5	Steel
pu-sol-therm-032-015	10.0	Pu(NO3)4	Annular	Water/Water	700.7	Steel
pu-sol-therm-032-016	10.0	Pu(NO3)4	Annular	Water/Water	800.5	Steel
pu-sol-therm-032-017	10.0	Pu(NO3)4	Annular	Water/Water	850.5	Steel
pu-sol-therm-034-001	8.3	Pu(NO3)4	Cylinder	Water/Water	230.1	Steel
pu-sol-therm-034-002	8.3	Pu(NO3)4	Cylinder	Water/Water	230.1	Steel, Gd
pu-sol-therm-034-003	8.3	Pu(NO3)4	Cylinder	Water/Water	230.1	Steel, Gd
pu-sol-therm-034-004	8.3	Pu(NO3)4	Cylinder	Water/Water	230.1	Steel, Gd
pu-sol-therm-034-005	8.3	Pu(NO3)4	Cylinder	Water/Water	230.1	Steel, Gd
pu-sol-therm-034-006	8.3	Pu(NO3)4	Cylinder	Water/Water	230.1	Steel, Gd
pu-sol-therm-034-007	8.3	Pu(NO3)4	Cylinder	Water/Water	59.1	Steel, Gd
pu-sol-therm-034-008	8.3	Pu(NO3)4	Cylinder	Water/Water	59.1	Steel, Gd
pu-sol-therm-034-009	8.3	Pu(NO3)4	Cylinder	Water/Water	59.1	Steel, Gd
pu-sol-therm-034-010	8.3	Pu(NO3)4	Cylinder	Water/Water	59.1	Steel, Gd
pu-sol-therm-034-011	8.3	Pu(NO3)4	Cylinder	Water/Water	59.1	Steel, Gd
pu-sol-therm-034-012	8.3	Pu(NO3)4	Cylinder	Water/Water	59.1	Steel, Gd
pu-sol-therm-034-013	8.3	Pu(NO3)4	Cylinder	Water/Water	59.1	Steel, Gd
pu-sol-therm-034-014	8.3	Pu(NO3)4	Cylinder	Water/Water	59.1	Steel, Gd
pu-sol-therm-034-015	8.3	Pu(NO3)4	Cylinder	Water/Water	59.1	Steel, Gd
pu-sol-therm-038-001	20.8	Pu(NO3)4	Cylinder	Water/Water	1701.6	Steel
pu-sol-therm-038-002	20.8	Pu(NO3)4	Cylinder	Water/Water	1664.5	Steel
pu-sol-therm-038-003	20.8	Pu(NO3)4	Cylinder	Water/Water	2234.1	Steel
pu-sol-therm-038-004	20.8	Pu(NO3)4	Cylinder	Water/Water	2355.9	Steel
pu-sol-therm-038-005	20.8	Pu(NO3)4	Cylinder	Water/Water	2347.1	Steel

APPENDIX 3: NORMALITY TESTS

The following tables provide the results of the normality tests applied to the complete set of benchmark data. Following the tables, the results of normality tests applied individually to three material form subsets are summarized.

Table 8 Modified Chi Square Normality Test Results for Entire Data Set

Class	Ordered Data	Class	Class Midpoint Mj	Occurrence Frequency Oj	$O_j \cdot M_j/n$	$O_j \cdot (M_j)^2/n$	
1	0.9922	1	0.99425	7	0.02667	0.02651	
1	0.9935	2	0.99875	50	0.19133	0.19109	
1	0.9937	3	1.00325	91	0.34979	0.35093	
1	0.9944	4	1.00775	66	0.25483	0.25681	
1	0.9944	5	1.01225	18	0.06981	0.07067	
1	0.9955	6	1.01675	9	0.03506	0.03565	
1	0.9961	7	1.02125	6	0.02348	0.02398	
2	0.9967	8	1.02575	6	0.02358	0.02419	
2	0.9967	9	1.03025	8	0.03158	0.03253	
2	0.9969						
2	0.9969		**Total**	261	1.00613	1.01235	
2	0.9970						
2	0.9971		**Estimated**	**Estimated**	**Estimated**		
2	0.9971		**Mean**	**Variance**	**S.D.**		
2	0.9974		1.00613	0.00006	0.00750		
2	0.9974						
2	0.9980		p1=Pr(0.992≤X<0.9965)				
2	0.9981	=	0.099443933	-	0.029709608		
2	0.9983	=	0.069734325				
2	0.9984	E1=	np1=	18.2006588			
2	0.9986						
2	0.9987		p2=Pr(0.9965≤X<1.001)				
2	0.9987	=	0.246869398	-	0.099467253		
2	0.9987	=	0.147402146				
2	0.9988	E2=	np2=	38.47195998			
2	0.9988						
2	0.9989		p3=Pr(1.001≤X<1.0055)				
2	0.9989	=	0.466519386	-	0.246911512		
2	0.9989	=	0.219607875				
2	0.9990	E3=	np3=	57.31765527			
2	0.9990						
2	0.9992		p4=Pr(1.0055≤X<1.01)				
2	0.9992	=	0.697188008	-	0.466572423		
2	0.9994	=	0.230615586				
2	0.9994	E4=	np4=	60.19066785			
2	0.9995						
2	0.9996		p5=Pr(1.01≤X<1.0145)				
2	0.9996	=	0.867934864	-	0.697234588		
2	0.9996	=	0.170700276				
2	0.9999	E5=	np5=	44.55277205			
2	1.0001						
2	1.0002		p6=Pr(1.0145≤X<1.019)				
2	1.0002	=	0.957013544	-	0.867963393		
2	1.0003	=	0.089050151				
2	1.0003	E6=	np6=	23.2420893			
2	1.0004						
2	1.0005		p7=Pr(1.019≤X<1.0235)				
2	1.0006	=	0.989758654	-	0.95702573		
2	1.0006	=	0.032732924				
2	1.0007	E7=	np7=	8.543293245			

2	1.0007						
2	1.0008		p8=Pr(1.0235≤X<1.028)				
2	1.0008	=	0.998237101	-	0.989762284		
2	1.0009	=	0.008474817				
2	1.0009	E8=	np8=	2.21192717			
2	1.0010						
2	1.0010		p9=Pr(1.028≤X<1.0325)				
3	1.0011	=	0.999782668	-	0.998237855		
3	1.0011	=	0.001544813				
3	1.0012	E9=	np9=	0.403196229			
3	1.0013						
3	1.0013						
3	1.0013						
3	1.0014						
3	1.0015						
3	1.0016						
3	1.0017						
3	1.0017						
3	1.0018						
3	1.0018						
3	1.0019						
3	1.0019						
3	1.0019						
3	1.0019						
3	1.0020						
3	1.0020						
3	1.0021						
3	1.0021		**c**				
3	1.0022	**χ^2*=**	**Σ**	**$(O_j)^2$**			
3	1.0022		**j=1**	**E_j**			
3	1.0023						
3	1.0024	**Class**	**Boundaries**	**O_j**	**$(O_j)^2$**	**E_j**	**$(O_j)^2/E_j$**
3	1.0025	1	0.99200 - 0.99650	7	49	18.20066	2.69221
3	1.0025	2	0.99650 - 1.00100	50	2500	38.47196	64.98239
3	1.0025	3	1.00100 - 1.00550	91	8281	57.31766	144.4756
3	1.0025	4	1.00550 - 1.01000	66	4356	60.19067	72.37002
3	1.0025	5	1.01000 - 1.01450	18	324	44.55277	7.272275
3	1.0027	6	1.01450 - 1.01900	9	81	23.24209	3.485057
3	1.0027	7	1.01900 - 1.02350	6	36	8.54329	4.213832
3	1.0027	8	1.02350 - 1.02800	6	36	2.21193	16.2754
3	1.0027	9	1.02800 - 1.03250	8	64	0.40320	158.7316
3	1.0028						
3	1.0028	**χ^2*=**	213.4983861				
3	1.0028						
3	1.0029	**$\chi^2(6)$=**	12.6 for α=0.05				
3	1.0029						
3	1.0029	**Since χ^2* > χ^2(9-2-1 = 6), reject the hypothesis that the data are from a normal distribution**					
3	1.0030						
3	1.0031						
3	1.0031						
3	1.0031						
3	1.0032						
3	1.0034						
3	1.0034						
3	1.0035						
3	1.0036						
3	1.0037						
3	1.0037						
3	1.0038						
3	1.0038						
3	1.0038						
3	1.0039						
3	1.0039						

3	1.0040						
3	1.0040						
3	1.0040						
3	1.0040						
3	1.0041						
3	1.0041						
3	1.0042						
3	1.0042						
3	1.0042						
3	1.0042						
3	1.0043						
3	1.0043						
3	1.0044						
3	1.0044						
3	1.0044						
3	1.0044						
3	1.0045						
3	1.0045						
3	1.0045						
3	1.0045						
3	1.0047						
3	1.0048						
3	1.0048						
3	1.0049						
3	1.0050						
3	1.0050						
3	1.0050						
3	1.0050						
3	1.0051						
3	1.0052						
3	1.0052						
3	1.0054						
3	1.0054						
3	1.0055						
3	1.0055						
4	1.0056						
4	1.0056						
4	1.0058						
4	1.0059						
4	1.0059						
4	1.0060						
4	1.0060						
4	1.0063						
4	1.0064						
4	1.0064						
4	1.0064						
4	1.0064						
4	1.0065						
4	1.0065						
4	1.0065						
4	1.0067						
4	1.0068						
4	1.0068						
4	1.0068						
4	1.0069						
4	1.0069						
4	1.0070						
4	1.0070						
4	1.0071						
4	1.0074						
4	1.0074						
4	1.0076						
4	1.0076						
4	1.0077						

4	1.0077						
4	1.0079						
4	1.0079						
4	1.0079						
4	1.0080						
4	1.0081						
4	1.0082						
4	1.0083						
4	1.0085						
4	1.0087						
4	1.0088						
4	1.0089						
4	1.0089						
4	1.0090						
4	1.0090						
4	1.0091						
4	1.0091						
4	1.0091						
4	1.0092						
4	1.0092						
4	1.0093						
4	1.0093						
4	1.0094						
4	1.0094						
4	1.0095						
4	1.0096						
4	1.0096						
4	1.0096						
4	1.0096						
4	1.0097						
4	1.0097						
4	1.0098						
4	1.0099						
4	1.0099						
4	1.0100						
4	1.0100						
4	1.0100						
5	1.0101						
5	1.0104						
5	1.0105						
5	1.0105						
5	1.0107						
5	1.0109						
5	1.0111						
5	1.0113						
5	1.0116						
5	1.0116						
5	1.0117						
5	1.0120						
5	1.0121						
5	1.0126						
5	1.0126						
5	1.0127						
5	1.0130						
5	1.0132						
6	1.0146						
6	1.0147						
6	1.0147						
6	1.0154						
6	1.0156						
6	1.0160						
6	1.0165						
6	1.0168						
6	1.0180						

7	1.0192						
7	1.0194						
7	1.0200						
7	1.0228						
7	1.0230						
7	1.0235						
8	1.0248						
8	1.0254						
8	1.0259						
8	1.0260						
8	1.0262						
8	1.0276						
9	1.0283						
9	1.0297						
9	1.0299						
9	1.0302						
9	1.0307						
9	1.0314						
9	1.0320						
9	1.0324						
	261						

Table 9 Kolmogorov-Smirnov Normality Test Results for Entire Data Set

Observation #	Ordered Data	$G(x_i)$	$F^*(x_i)$	$[F^*(x_i) - G(x_i)]$	$[F^*(x_i) - G(x_{i-1})]$	$T^* = \sup[F^*(x) - G(x)]$	$w_{95}(261)$
1	0.9922	0.0038	0.0428	0.0389	0.0428	0.2174	0.0842
2	0.9935	0.0077	0.0565	0.0489	0.0527	**Since $T^* > w_{95}(261)$, reject the hypothesis that**	
3	0.9937	0.0115	0.0591	0.0476	0.0514	**the data are from a normal distribution**	
4	0.9944	0.0153	0.0690	0.0537	0.0575		
5							
6	0.9955	0.0230	0.0869	0.0640	0.0716		
7	0.9961	0.0268	0.0988	0.0720	0.0758		
8							
9	0.9967	0.0345	0.1105	0.0760	0.0837		
10							
11	0.9969	0.0421	0.1159	0.0737	0.0814		
12	0.9970	0.0460	0.1162	0.0703	0.0741		
13							
14	0.9971	0.0536	0.1191	0.0655	0.0731		
15							
16	0.9974	0.0613	0.1266	0.0653	0.0729		
17	0.9980	0.0651	0.1405	0.0753	0.0792		
18	0.9981	0.0690	0.1432	0.0743	0.0781		
19	0.9983	0.0728	0.1491	0.0763	0.0801		
20	0.9984	0.0766	0.1509	0.0743	0.0781		
21	0.9986	0.0805	0.1570	0.0765	0.0804		
22							
23							
24	0.9987	0.0920	0.1589	0.0669	0.0784		
25							
26	0.9988	0.0996	0.1618	0.0622	0.0699		
27							
28							
29	0.9989	0.1111	0.1651	0.0540	0.0655		
30							
31	0.9990	0.1188	0.1679	0.0491	0.0568		
32							
33	0.9992	0.1264	0.1733	0.0468	0.0545		
34							
35	0.9994	0.1341	0.1785	0.0444	0.1785		
36	0.9995	0.1379	0.1796	0.0417	0.0455		
37							
38							
39	0.9996	0.1494	0.1852	0.0358	0.0473		
40	0.9999	0.1533	0.1937	0.0404	0.0442		
41	1.0001	0.1571	0.2005	0.0434	0.0472		
42							
43	1.0002	0.1648	0.2023	0.0376	0.0453		
44							
45	1.0003	0.1724	0.2061	0.0337	0.0414		
46	1.0004	0.1762	0.2080	0.0318	0.0356		
47	1.0005	0.1801	0.2106	0.0305	0.0344		
48							
49	1.0006	0.1877	0.2164	0.0287	0.0364		
50							
51	1.0007	0.1954	0.2197	0.0243	0.0320		
52							
53	1.0008	0.2031	0.2230	0.0200	0.0276		
54							
55	1.0009	0.2107	0.2257	0.0150	0.0226		
56							
57	1.0010	0.2184	0.2290	0.0107	0.0183		
58							
59	1.0011	0.2261	0.2328	0.0067	0.0144		

60	1.0012	0.2299	0.2358	0.0060	0.0098		
61							
62							
63	1.0013	0.2414	0.2396	0.0017	0.0097		
64	1.0014	0.2452	0.2418	0.0034	0.0004		
65	1.0015	0.2490	0.2438	0.0052	0.0014		
66	1.0016	0.2529	0.2490	0.0038	0.0000		
67							
68	1.0017	0.2605	0.2537	0.0069	0.0008		
69							
70	1.0018	0.2682	0.2558	0.0124	0.0047		
71							
72							
73							
74	1.0019	0.2835	0.2604	0.0231	0.0078		
75							
76	1.0020	0.2912	0.2645	0.0267	0.0190		
77							
78	1.0021	0.2989	0.2667	0.0322	0.0245		
79							
80	1.0022	0.3065	0.2702	0.0364	0.0287		
81	1.0023	0.3103	0.2737	0.0367	0.0328		
82	1.0024	0.3142	0.2766	0.0375	0.0337		
83							
84							
85							
86							
87	1.0025	0.3333	0.2826	0.0507	0.0315		
88							
89							
90							
91	1.0027	0.3487	0.2898	0.0588	0.0435		
92							
93							
94	1.0028	0.3602	0.2948	0.0654	0.0539		
95							
96							
97	1.0029	0.3716	0.2967	0.0749	0.0634		
98	1.0030	0.3755	0.2998	0.0757	0.0718		
99							
100							
101	1.0031	0.3870	0.3064	0.0805	0.0690		
102	1.0032	0.3908	0.3096	0.0812	0.0774		
103							
104	1.0034	0.3985	0.3175	0.0810	0.0733		
105	1.0035	0.4023	0.3202	0.0821	0.0782		
106	1.0036	0.4061	0.3250	0.0811	0.0773		
107							
108	1.0037	0.4138	0.3290	0.0847	0.0771		
109							
110							
111	1.0038	0.4253	0.3331	0.0922	0.0807		
112							
113	1.0039	0.4330	0.3380	0.0950	0.0873		
114							
115							
116							
117	1.0040	0.4483	0.3420	0.1062	0.0909		
118							
119	1.0041	0.4559	0.3453	0.1106	0.1030		
120							
121							
122							
123	1.0042	0.4713	0.3507	0.1206	0.1053		

124							
125	1.0043	0.4789	0.3536	0.1254	0.1177		
126							
127							
128							
129	1.0044	0.4943	0.3589	0.1353	0.1200		
130							
131							
132							
133	1.0045	0.5096	0.3631	0.1465	0.1311		
134	1.0047	0.5134	0.3690	0.1444	0.1406		
135							
136	1.0048	0.5211	0.3744	0.1466	0.1390		
137	1.0049	0.5249	0.3761	0.1488	0.1449		
138							
139							
140							
141	1.0050	0.5402	0.3833	0.1569	0.1416		
142	1.0051	0.5441	0.3885	0.1556	0.1518		
143							
144	1.0052	0.5517	0.3927	0.1590	0.1513		
145							
146	1.0054	0.5594	0.4009	0.1585	0.1508		
147							
148	1.0055	0.5670	0.4035	0.1636	0.1559		
149							
150	1.0056	0.5747	0.4082	0.1665	0.1588		
151	1.0058	0.5785	0.4164	0.1621	0.1583		
152							
153	1.0059	0.5862	0.4230	0.1632	0.1556		
154							
155	1.0060	0.5939	0.4256	0.1683	0.1606		
156	1.0063	0.5977	0.4392	0.1585	0.1547		
157							
158							
159							
160	1.0064	0.6130	0.4440	0.1690	0.1537		
161							
162							
163	1.0065	0.6245	0.4488	0.1757	0.1642		
164	1.0067	0.6284	0.4572	0.1711	0.1673		
165							
166							
167	1.0068	0.6398	0.4625	0.1773	0.1658		
168							
169	1.0069	0.6475	0.4665	0.1810	0.1734		
170							
171	1.0070	0.6552	0.4683	0.1869	0.1792		
172	1.0071	0.6590	0.4749	0.1841	0.1803		
173							
174	1.0074	0.6667	0.4869	0.1798	0.1721		
175							
176	1.0076	0.6743	0.4958	0.1786	0.1709		
177							
178	1.0077	0.6820	0.4998	0.1822	0.1746		
179							
180							
181	1.0079	0.6935	0.5113	0.1822	0.1707		
182	1.0080	0.6973	0.5149	0.1825	0.1786		
183	1.0081	0.7011	0.5166	0.1845	0.1807		
184	1.0082	0.7050	0.5246	0.1804	0.1765		
185	1.0083	0.7088	0.5255	0.1833	0.1795		
186	1.0085	0.7126	0.5375	0.1752	0.1713		
187	1.0087	0.7165	0.5453	0.1711	0.1673		

188	1.0088	0.7203	0.5503	0.1701	0.1662		
189							
190	1.0089	0.7280	0.5525	0.1755	0.1679		
191							
192	1.0090	0.7356	0.5577	0.1779	0.1702		
193							
194							
195	1.0091	0.7471	0.5634	0.1837	0.1722		
196							
197	1.0092	0.7548	0.5656	0.1892	0.1815		
198							
199	1.0093	0.7625	0.5713	0.1911	0.1835		
200							
201	1.0094	0.7701	0.5774	0.1927	0.1850		
202	1.0095	0.7739	0.5789	0.1950	0.1912		
203							
204							
205							
206	1.0096	0.7893	0.5857	0.2036	0.1883		
207							
208	1.0097	0.7969	0.5879	0.2091	0.2014		
209	1.0098	0.8008	0.5918	0.2090	0.2052		
210							
211	1.0099	0.8084	0.5974	0.2111	0.2034		
212							
213							
214	1.0100	0.8199	0.6030	0.2169	0.2054		
215	1.0101	0.8238	0.6064	0.2174	0.2135		
216	1.0104	0.8276	0.6189	0.2087	0.2049		
217							
218	1.0105	0.8352	0.6251	0.2102	0.2025		
219	1.0107	0.8391	0.6318	0.2073	0.2034		
220	1.0109	0.8429	0.6410	0.2019	0.1981		
221	1.0111	0.8467	0.6481	0.1987	0.1948		
222	1.0113	0.8506	0.6573	0.1933	0.1895		
223							
224	1.0116	0.8582	0.6693	0.1889	0.1813		
225	1.0117	0.8621	0.6713	0.1907	0.1869		
226	1.0120	0.8659	0.6863	0.1796	0.1758		
227	1.0121	0.8697	0.6882	0.1815	0.1777		
228							
229	1.0126	0.8774	0.7086	0.1688	0.1611		
230	1.0127	0.8812	0.7111	0.1701	0.1663		
231	1.0130	0.8851	0.7239	0.1612	0.1573		
232	1.0132	0.8889	0.7318	0.1571	0.1532		
233	1.0146	0.8927	0.7776	0.1151	0.1113		
234							
235	1.0147	0.9004	0.7839	0.1165	0.1089		
236	1.0154	0.9042	0.8040	0.1002	0.0964		
237	1.0156	0.9080	0.8101	0.0979	0.0941		
238	1.0160	0.9119	0.8224	0.0895	0.0857		
239	1.0165	0.9157	0.8379	0.0779	0.0740		
240	1.0168	0.9195	0.8457	0.0739	0.0701		
241	1.0180	0.9234	0.8746	0.0488	0.0450		
242	1.0192	0.9272	0.9004	0.0268	0.0229		
243	1.0194	0.9310	0.9041	0.0269	0.0231		
244	1.0200	0.9349	0.9152	0.0197	0.0159		
245	1.0228	0.9387	0.9536	0.0149	0.0187		
246	1.0230	0.9425	0.9558	0.0133	0.0171		
247	1.0235	0.9464	0.9612	0.0149	0.0187		
248	1.0248	0.9502	0.9719	0.0218	0.0256		
249	1.0254	0.9540	0.9757	0.0217	0.0255		
250	1.0259	0.9579	0.9787	0.0208	0.0247		
251	1.0260	0.9617	0.9790	0.0173	0.0211		

252	1.0262	0.9655	0.9802	0.0147	0.0185		
253	1.0276	0.9693	0.9866	0.0173	0.0211		
254	1.0283	0.9732	0.9891	0.0159	0.0197		
255	1.0297	0.9770	0.9928	0.0157	0.0196		
256	1.0299	0.9808	0.9932	0.0124	0.0162		
257	1.0302	0.9847	0.9939	0.0092	0.0130		
258	1.0307	0.9885	0.9948	0.0063	0.0101		
259	1.0314	0.9923	0.9958	0.0035	0.0073		
260	1.0320	0.9962	0.9966	0.0004	0.0043		
261	1.0324	1.0000	0.9970	0.0030	0.0008		
$\overline{x_i}$	1.0077						
σ	0.0090						

Table 10 Lilliefors Normality Test Results for Entire Data Set

Observation #	x_i	z_i	$F^*(z_i)$	$G(z_i)$	$\lvert F^*(z_i) - G(z_i)\rvert$	$\lvert F^*(z_i) - G(z_{i-1})\rvert$	T*	$w_{95}(261)$
1	0.99224	-1.861	0.03137	0.0038	0.0275	0.0314	0.1266	0.054842
2	0.99345	-1.700	0.04456	0.0077	0.0369	0.0407	**Since T* > $w_{95}(261)$, reject the hypothesis that the data are from a normal distribution**	
3	0.99365	-1.674	0.04712	0.0115	0.0356	0.0395		
4	0.99436	-1.579	0.05717	0.0153	0.0418	0.0457		
5	0.99444	-1.568	0.05840	0.0192	0.0392	0.0431		
6	0.99547	-1.431	0.07616	0.0230	0.0532	0.0570		
7	0.99611	-1.346	0.08911	0.0268	0.0623	0.0661		
8	0.99665	-1.274	0.10125	0.0307	0.0706	0.0744		
9	0.99669	-1.269	0.10219	0.0345	0.0677	0.0715		
10	0.99687	-1.245	0.10653	0.0383	0.0682	0.0720		
11	0.99694	-1.236	0.10831	0.0421	0.0662	0.0700		
12	0.99696	-1.233	0.10874	0.0460	0.0628	0.0666		
13	0.99708	-1.217	0.11175	0.0498	0.0619	0.0658		
14	0.99709	-1.216	0.11200	0.0536	0.0584	0.0622		
15	0.99735	-1.181	0.11873	0.0575	0.0613	0.0651		
16	0.99742	-1.172	0.12058	0.0613	0.0593	0.0631		
17	0.99800	-1.095	0.13677	0.0651	0.0716	0.0755		
18	0.99811	-1.080	0.14001	0.0690	0.0710	0.0749		
19	0.99834	-1.050	0.14693	0.0728	0.0741	0.0780		
20	0.99841	-1.040	0.14908	0.0766	0.0725	0.0763		
21	0.99864	-1.010	0.15630	0.0805	0.0758	0.0797		
22	0.99866	-1.007	0.15694	0.0843	0.0726	0.0765		
23	0.99866	-1.007	0.15694	0.0881	0.0688	0.0726		
24	0.99871	-1.000	0.15854	0.0920	0.0666	0.0704		
25	0.99878	-0.991	0.16080	0.0958	0.0650	0.0688		
26	0.99882	-0.986	0.16211	0.0996	0.0625	0.0663		
27	0.99885	-0.982	0.16309	0.1034	0.0596	0.0635		
28	0.99885	-0.982	0.16309	0.1073	0.0558	0.0596		
29	0.99894	-0.970	0.16603	0.1111	0.0549	0.0588		
30	0.99895	-0.968	0.16639	0.1149	0.0514	0.0553		
31	0.99904	-0.957	0.16939	0.1188	0.0506	0.0545		
32	0.99919	-0.937	0.17448	0.1226	0.0519	0.0557		
33	0.99923	-0.931	0.17585	0.1264	0.0494	0.0532		
34	0.99938	-0.911	0.18106	0.1303	0.0508	0.0546		
35	0.99941	-0.907	0.18211	0.1341	0.0480	0.0518		
36	0.99945	-0.902	0.18352	0.1379	0.0456	0.0494		
37	0.99963	-0.878	0.18995	0.1418	0.0482	0.0520		
38	0.99964	-0.877	0.19032	0.1456	0.0447	0.0486		
39	0.99964	-0.877	0.19032	0.1494	0.0409	0.0447		
40	0.99992	-0.839	0.20060	0.1533	0.0473	0.0512		
41	1.00014	-0.810	0.20891	0.1571	0.0518	0.0557		
42	1.00015	-0.809	0.20929	0.1609	0.0484	0.0522		
43	1.00020	-0.802	0.21121	0.1648	0.0465	0.0503		
44	1.00025	-0.796	0.21314	0.1686	0.0446	0.0484		
45	1.00032	-0.786	0.21586	0.1724	0.0434	0.0473		
46	1.00038	-0.778	0.21821	0.1762	0.0420	0.0458		
47	1.00046	-0.768	0.22136	0.1801	0.0413	0.0451		
48	1.00057	-0.753	0.22573	0.1839	0.0418	0.0457		
49	1.00064	-0.744	0.22854	0.1877	0.0408	0.0446		
50	1.00068	-0.738	0.23015	0.1916	0.0386	0.0424		
51	1.00074	-0.730	0.23258	0.1954	0.0372	0.0410		
52	1.00080	-0.722	0.23503	0.1992	0.0358	0.0396		
53	1.00084	-0.717	0.23667	0.2031	0.0336	0.0374		
54	1.00085	-0.716	0.23708	0.2069	0.0302	0.0340		
55	1.00092	-0.706	0.23997	0.2107	0.0292	0.0331		
56	1.00096	-0.701	0.24162	0.2146	0.0271	0.0309		
57	1.00102	-0.693	0.24412	0.2184	0.0257	0.0296		
58	1.00108	-0.685	0.24663	0.2222	0.0244	0.0282		
59	1.00113	-0.679	0.24871	0.2261	0.0227	0.0265		

60	1.00122	-0.666	0.25255	0.2299	0.0227	0.0265		
61	1.00129	-0.657	0.25553	0.2337	0.0218	0.0256		
62	1.00129	-0.657	0.25553	0.2375	0.0180	0.0218		
63	1.00133	-0.652	0.25725	0.2414	0.0159	0.0197		
64	1.00139	-0.643	0.25997	0.2452	0.0148	0.0186		
65	1.00145	-0.636	0.26242	0.2490	0.0134	0.0172		
66	1.00160	-0.616	0.26894	0.2529	0.0161	0.0199		
67	1.00165	-0.609	0.27134	0.2567	0.0146	0.0185		
68	1.00173	-0.599	0.27471	0.2605	0.0142	0.0180		
69	1.00175	-0.596	0.27566	0.2644	0.0113	0.0151		
70	1.00179	-0.591	0.27738	0.2682	0.0092	0.0130		
71	1.00186	-0.581	0.28051	0.2720	0.0085	0.0123		
72	1.00188	-0.579	0.28141	0.2759	0.0055	0.0094		
73	1.00190	-0.576	0.28224	0.2797	0.0026	0.0064		
74	1.00192	-0.574	0.28313	0.2835	0.0004	0.0034		
75	1.00195	-0.569	0.28473	0.2874	0.0026	0.0012		
76	1.00203	-0.559	0.28818	0.2912	0.0030	0.0008		
77	1.00209	-0.551	0.29091	0.2950	0.0041	0.0003		
78	1.00209	-0.551	0.29091	0.2989	0.0079	0.0041		
79	1.00216	-0.541	0.29411	0.3027	0.0086	0.0047		
80	1.00218	-0.538	0.29525	0.3065	0.0113	0.0074		
81	1.00228	-0.525	0.29964	0.3103	0.0107	0.0069		
82	1.00236	-0.515	0.30335	0.3142	0.0108	0.0070		
83	1.00247	-0.500	0.30848	0.3180	0.0095	0.0057		
84	1.00248	-0.499	0.30895	0.3218	0.0129	0.0091		
85	1.00250	-0.496	0.30989	0.3257	0.0158	0.0120		
86	1.00251	-0.495	0.31036	0.3295	0.0191	0.0153		
87	1.00252	-0.494	0.31083	0.3333	0.0225	0.0187		
88	1.00266	-0.475	0.31743	0.3372	0.0197	0.0159		
89	1.00267	-0.474	0.31791	0.3410	0.0231	0.0193		
90	1.00271	-0.468	0.31981	0.3448	0.0250	0.0212		
91	1.00271	-0.468	0.31981	0.3487	0.0288	0.0250		
92	1.00279	-0.458	0.32345	0.3525	0.0290	0.0252		
93	1.00283	-0.452	0.32554	0.3563	0.0308	0.0270		
94	1.00284	-0.451	0.32595	0.3602	0.0342	0.0304		
95	1.00286	-0.448	0.32698	0.3640	0.0370	0.0332		
96	1.00288	-0.446	0.32794	0.3678	0.0399	0.0360		
97	1.00289	-0.444	0.32842	0.3716	0.0432	0.0394		
98	1.00297	-0.434	0.33228	0.3755	0.0432	0.0394		
99	1.00313	-0.413	0.33997	0.3793	0.0393	0.0355		
100	1.00313	-0.413	0.33997	0.3831	0.0432	0.0393		
101	1.00314	-0.411	0.34053	0.3870	0.0464	0.0426		
102	1.00322	-0.400	0.34444	0.3908	0.0464	0.0425		
103	1.00335	-0.383	0.35083	0.3946	0.0438	0.0400		
104	1.00342	-0.374	0.35429	0.3985	0.0442	0.0403		
105	1.00349	-0.364	0.35776	0.4023	0.0445	0.0407		
106	1.00361	-0.349	0.36374	0.4061	0.0424	0.0386		
107	1.00366	-0.342	0.36624	0.4100	0.0437	0.0399		
108	1.00371	-0.335	0.36874	0.4138	0.0450	0.0412		
109	1.00375	-0.330	0.37075	0.4176	0.0469	0.0430		
110	1.00381	-0.322	0.37377	0.4215	0.0477	0.0439		
111	1.00381	-0.322	0.37377	0.4253	0.0515	0.0477		
112	1.00388	-0.313	0.37709	0.4291	0.0520	0.0482		
113	1.00393	-0.306	0.37984	0.4330	0.0531	0.0493		
114	1.00395	-0.303	0.38085	0.4368	0.0559	0.0521		
115	1.00397	-0.301	0.38186	0.4406	0.0588	0.0549		
116	1.00401	-0.295	0.38389	0.4444	0.0606	0.0567		
117	1.00403	-0.293	0.38491	0.4483	0.0634	0.0595		
118	1.00407	-0.287	0.38695	0.4521	0.0652	0.0613		
119	1.00411	-0.282	0.38898	0.4559	0.0670	0.0631		
120	1.00415	-0.277	0.39103	0.4598	0.0687	0.0649		
121	1.00418	-0.273	0.39256	0.4636	0.0710	0.0672		
122	1.00421	-0.269	0.39409	0.4674	0.0733	0.0695		
123	1.00424	-0.265	0.39563	0.4713	0.0756	0.0718		

124	1.00430	-0.257	0.39871	0.4751	0.0764	0.0726		
125	1.00431	-0.255	0.39922	0.4789	0.0797	0.0759		
126	1.00441	-0.242	0.40437	0.4828	0.0784	0.0746		
127	1.00442	-0.241	0.40488	0.4866	0.0817	0.0779		
128	1.00443	-0.239	0.40540	0.4904	0.0850	0.0812		
129	1.00444	-0.238	0.40592	0.4943	0.0883	0.0845		
130	1.00446	-0.235	0.40695	0.4981	0.0911	0.0873		
131	1.00450	-0.230	0.40901	0.5019	0.0929	0.0891		
132	1.00451	-0.229	0.40953	0.5057	0.0962	0.0924		
133	1.00454	-0.225	0.41108	0.5096	0.0985	0.0947		
134	1.00468	-0.206	0.41834	0.5134	0.0951	0.0912		
135	1.00476	-0.196	0.42250	0.5172	0.0947	0.0909		
136	1.00481	-0.189	0.42511	0.5211	0.0960	0.0921		
137	1.00485	-0.184	0.42719	0.5249	0.0977	0.0939		
138	1.00497	-0.168	0.43347	0.5287	0.0953	0.0914		
139	1.00499	-0.165	0.43467	0.5326	0.0979	0.0941		
140	1.00500	-0.164	0.43504	0.5364	0.1014	0.0975		
141	1.00502	-0.161	0.43608	0.5402	0.1041	0.1003		
142	1.00514	-0.145	0.44238	0.5441	0.1017	0.0979		
143	1.00520	-0.137	0.44553	0.5479	0.1024	0.0985		
144	1.00524	-0.132	0.44763	0.5517	0.1041	0.1003		
145	1.00539	-0.112	0.45554	0.5556	0.1000	0.0962		
146	1.00543	-0.106	0.45765	0.5594	0.1017	0.0979		
147	1.00549	-0.098	0.46081	0.5632	0.1024	0.0986		
148	1.00549	-0.098	0.46081	0.5670	0.1062	0.1024		
149	1.00558	-0.086	0.46557	0.5709	0.1053	0.1015		
150	1.00560	-0.084	0.46663	0.5747	0.1081	0.1043		
151	1.00579	-0.059	0.47668	0.5785	0.1019	0.0980		
152	1.00594	-0.039	0.48463	0.5824	0.0977	0.0939		
153	1.00594	-0.039	0.48463	0.5862	0.1016	0.0977		
154	1.00595	-0.037	0.48516	0.5900	0.1049	0.1010		
155	1.00600	-0.031	0.48782	0.5939	0.1061	0.1022		
156	1.00631	0.011	0.50429	0.5977	0.0934	0.0896		
157	1.00636	0.017	0.50692	0.6015	0.0946	0.0908		
158	1.00636	0.017	0.50692	0.6054	0.0984	0.0946		
159	1.00638	0.020	0.50798	0.6092	0.1012	0.0974		
160	1.00642	0.025	0.51010	0.6130	0.1029	0.0991		
161	1.00647	0.032	0.51275	0.6169	0.1041	0.1003		
162	1.00652	0.039	0.51541	0.6207	0.1053	0.1015		
163	1.00653	0.040	0.51594	0.6245	0.1086	0.1048		
164	1.00672	0.065	0.52600	0.6284	0.1023	0.0985		
165	1.00675	0.069	0.52759	0.6322	0.1046	0.1008		
166	1.00682	0.079	0.53130	0.6360	0.1047	0.1009		
167	1.00684	0.081	0.53235	0.6398	0.1075	0.1037		
168	1.00686	0.083	0.53319	0.6437	0.1105	0.1067		
169	1.00693	0.093	0.53711	0.6475	0.1104	0.1066		
170	1.00696	0.097	0.53870	0.6513	0.1126	0.1088		
171	1.00697	0.098	0.53923	0.6552	0.1159	0.1121		
172	1.00712	0.118	0.54714	0.6590	0.1119	0.1080		
173	1.00736	0.150	0.55980	0.6628	0.1030	0.0992		
174	1.00739	0.154	0.56133	0.6667	0.1053	0.1015		
175	1.00755	0.176	0.56971	0.6705	0.1008	0.0970		
176	1.00759	0.181	0.57180	0.6743	0.1025	0.0987		
177	1.00767	0.192	0.57597	0.6782	0.1022	0.0984		
178	1.00768	0.193	0.57649	0.6820	0.1055	0.1017		
179	1.00785	0.216	0.58533	0.6858	0.1005	0.0967		
180	1.00789	0.221	0.58740	0.6897	0.1023	0.0984		
181	1.00794	0.228	0.58999	0.6935	0.1035	0.0997		
182	1.00802	0.238	0.59412	0.6973	0.1032	0.0994		
183	1.00806	0.243	0.59618	0.7011	0.1050	0.1011		
184	1.00824	0.267	0.60543	0.7050	0.0996	0.0957		
185	1.00826	0.270	0.60645	0.7088	0.1024	0.0985		
186	1.00853	0.306	0.62021	0.7126	0.0924	0.0886		
187	1.00871	0.330	0.62921	0.7165	0.0873	0.0834		

188	1.00882	0.345	0.63479	0.7203	0.0855	0.0817		
189	1.00885	0.349	0.63629	0.7241	0.0878	0.0840		
190	1.00887	0.351	0.63729	0.7280	0.0907	0.0868		
191	1.00896	0.363	0.64177	0.7318	0.0900	0.0862		
192	1.00899	0.367	0.64326	0.7356	0.0924	0.0885		
193	1.00910	0.382	0.64870	0.7395	0.0908	0.0869		
194	1.00911	0.383	0.64920	0.7433	0.0941	0.0903		
195	1.00912	0.385	0.64969	0.7471	0.0974	0.0936		
196	1.00915	0.389	0.65129	0.7510	0.0997	0.0958		
197	1.00917	0.391	0.65215	0.7548	0.1026	0.0988		
198	1.00926	0.403	0.65656	0.7586	0.1021	0.0982		
199	1.00930	0.408	0.65852	0.7625	0.1039	0.1001		
200	1.00940	0.422	0.66339	0.7663	0.1029	0.0991		
201	1.00944	0.427	0.66533	0.7701	0.1048	0.1010		
202	1.00947	0.432	0.66701	0.7739	0.1069	0.1031		
203	1.00957	0.444	0.67160	0.7778	0.1062	0.1023		
204	1.00960	0.448	0.67304	0.7816	0.1086	0.1047		
205	1.00960	0.449	0.67327	0.7854	0.1122	0.1083		
206	1.00963	0.452	0.67448	0.7893	0.1148	0.1110		
207	1.00967	0.458	0.67640	0.7931	0.1167	0.1129		
208	1.00968	0.459	0.67687	0.7969	0.1201	0.1162		
209	1.00977	0.471	0.68116	0.8008	0.1196	0.1158		
210	1.00989	0.487	0.68684	0.8046	0.1178	0.1139		
211	1.00990	0.488	0.68731	0.8084	0.1211	0.1173		
212	1.01001	0.503	0.69248	0.8123	0.1198	0.1160		
213	1.01002	0.504	0.69294	0.8161	0.1231	0.1193		
214	1.01003	0.506	0.69346	0.8199	0.1265	0.1226		
215	1.01011	0.516	0.69714	0.8238	0.1266	0.1228		
216	1.01040	0.555	0.71062	0.8276	0.1170	0.1131		
217	1.01055	0.574	0.71709	0.8314	0.1143	0.1105		
218	1.01055	0.575	0.71723	0.8352	0.1180	0.1142		
219	1.01071	0.596	0.72441	0.8391	0.1147	0.1108		
220	1.01093	0.625	0.73407	0.8429	0.1088	0.1050		
221	1.01110	0.648	0.74147	0.8467	0.1053	0.1014		
222	1.01132	0.678	0.75102	0.8506	0.0996	0.0957		
223	1.01155	0.708	0.76045	0.8544	0.0940	0.0901		
224	1.01162	0.717	0.76333	0.8582	0.0949	0.0911		
225	1.01167	0.724	0.76538	0.8621	0.0967	0.0929		
226	1.01204	0.774	0.78040	0.8659	0.0855	0.0817		
227	1.01209	0.780	0.78236	0.8697	0.0874	0.0835		
228	1.01257	0.844	0.80056	0.8736	0.0730	0.0692		
229	1.01262	0.850	0.80237	0.8774	0.0750	0.0712		
230	1.01269	0.859	0.80477	0.8812	0.0765	0.0726		
231	1.01303	0.904	0.81702	0.8851	0.0680	0.0642		
232	1.01324	0.933	0.82449	0.8889	0.0644	0.0606		
233	1.01455	1.107	0.86582	0.8927	0.0269	0.0231		
234	1.01470	1.127	0.87008	0.8966	0.0265	0.0226		
235	1.01474	1.132	0.87121	0.9004	0.0292	0.0253		
236	1.01538	1.217	0.88812	0.9042	0.0161	0.0123		
237	1.01558	1.243	0.89311	0.9080	0.0149	0.0111		
238	1.01599	1.298	0.90292	0.9119	0.0090	0.0051		
239	1.01654	1.372	0.91489	0.9157	0.0008	0.0030		
240	1.01683	1.410	0.92074	0.9195	0.0012	0.0050		
241	1.01800	1.566	0.94129	0.9234	0.0179	0.0218		
242	1.01922	1.728	0.95801	0.9272	0.0308	0.0346		
243	1.01941	1.754	0.96026	0.9310	0.0292	0.0331		
244	1.02002	1.835	0.96674	0.9349	0.0319	0.0357		
245	1.02278	2.202	0.98619	0.9387	0.0475	0.0513		
246	1.02299	2.230	0.98714	0.9425	0.0446	0.0484		
247	1.02354	2.303	0.98938	0.9464	0.0430	0.0469		
248	1.02484	2.477	0.99336	0.9502	0.0432	0.0470		
249	1.02540	2.550	0.99460	0.9540	0.0406	0.0444		
250	1.02590	2.616	0.99553	0.9579	0.0377	0.0415		
251	1.02595	2.624	0.99562	0.9617	0.0339	0.0378		

252	1.02617	2.652	0.99597	0.9655	0.0305	0.0343		
253	1.02758	2.840	0.99770	0.9693	0.0284	0.0322		
254	1.02828	2.934	0.99829	0.9732	0.0251	0.0289		
255	1.02965	3.116	0.99908	0.9770	0.0221	0.0259		
256	1.02986	3.144	0.99917	0.9808	0.0183	0.0222		
257	1.03018	3.186	0.99929	0.9847	0.0146	0.0185		
258	1.03071	3.257	0.99946	0.9885	0.0110	0.0148		
259	1.03137	3.345	0.99961	0.9923	0.0073	0.0111		
260	1.03201	3.430	0.99971	0.9962	0.0035	0.0074		
261	1.03238	3.479	0.99975	1.0000	0.0002	0.0036		
$\overline{x_i}$	1.0062							
σ	0.0075							

To support the Section 6.2 evaluation of individual material form subsets (i.e., metal, oxide, and solution subsets), each of the three material form subsets was evaluated separately using the three normality tests described in Section 3.4.1. All three material form subsets failed the Chi Square test, while the solution subset also failed the Lilliefors test (the sample size for the oxide subset was too small to perform the Lilliefors test). The detailed results are not reproduced herein, but the Chi Square test histograms are presented below, in Figures 5 through 7.

Figure 5 Histogram of Metal Calculation Results

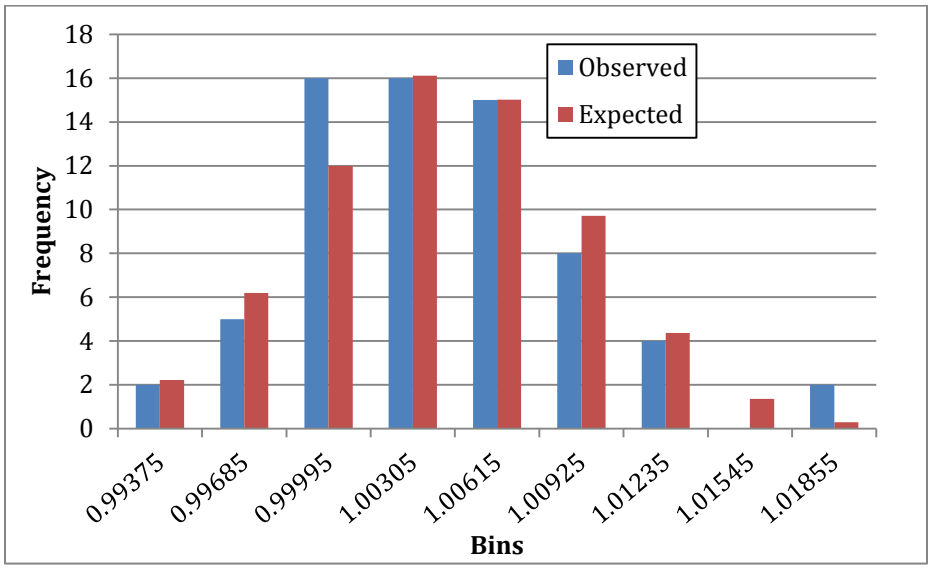

Figure 6 Histogram of Oxide Calculation Results

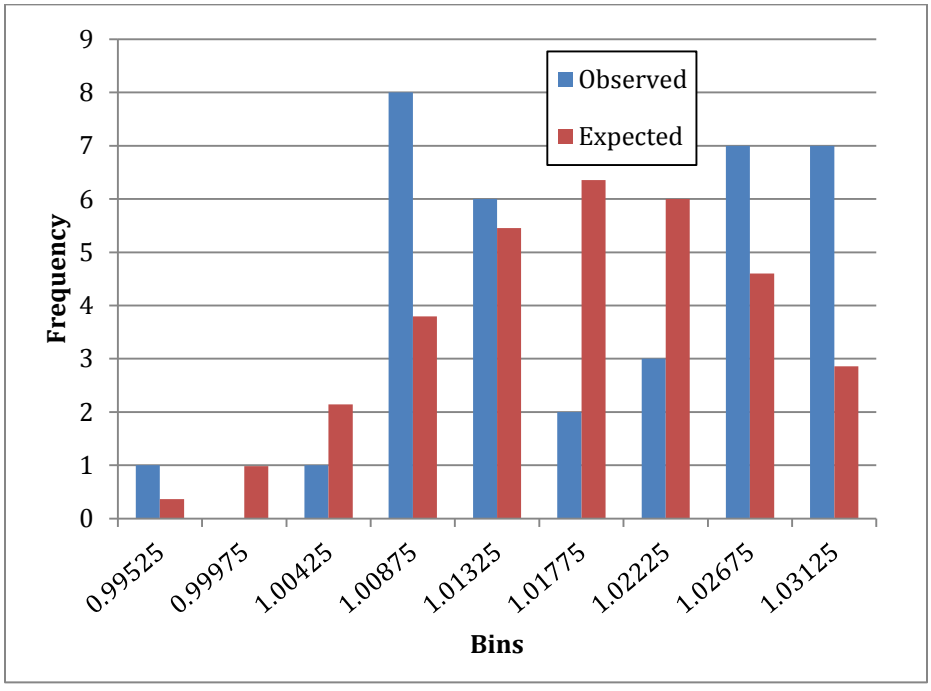

Figure 7 Histogram of Solution Calculation Results

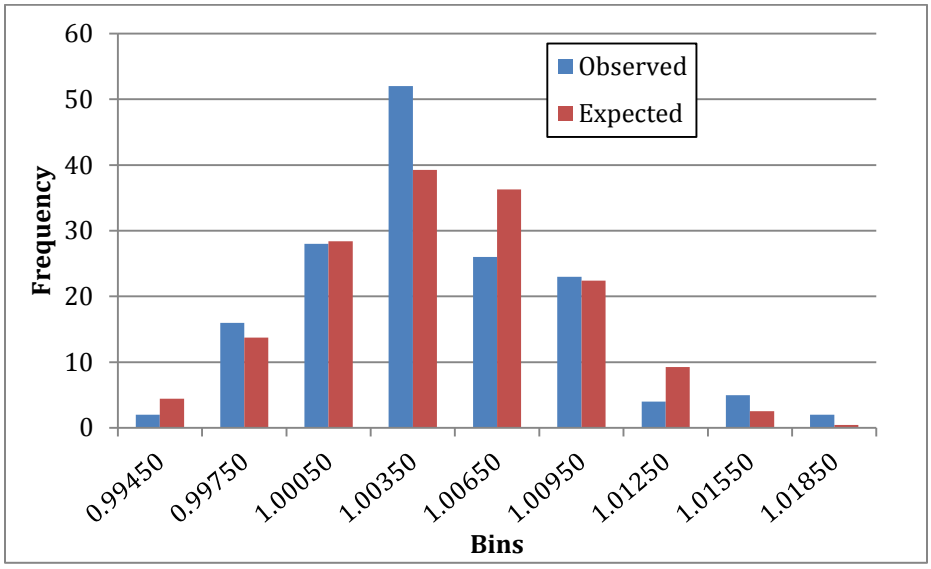

Based on the failure of any of the material form subsets to pass all three normality tests, and supported by visual inspection of the histograms above, it is concluded that these three material form subsets cannot be confirmed to come from a normal distribution.

APPENDIX 4: MATERIAL FORM SUBSET TRENDING ANALYSIS

In Section 4.4, the complete benchmark critical experiment data set was analyzed to determine if any trends existed between the calculated k_{eff} results and three important nuclear parameters: ^{240}Pu content, moderation ratio, and ANECF. In this appendix, the results of similar trending analyses applied to three individual material form subsets (i.e., metal, oxide, or solution) are presented.

Graphs of the benchmark results versus these parameters for each of the three material form subsets are presented as Figures 8 through 16. For each combination of material form subset and nuclear trending parameter, the attempted data fit resulting in the highest coefficient of determination value (R^2) is also depicted on the associated graph.

The highest R^2 value determined was 0.62, obtained for an attempted fit between the metal data and moderation ratio. Based on this low maximum R^2 value, along with visual inspections of Figures 8 through 16, it is concluded that the individual material form subsets do not correlate with any of the three nuclear parameters investigated.

Figure 8 ^{240}Pu wt% Trend Analysis (Metal)

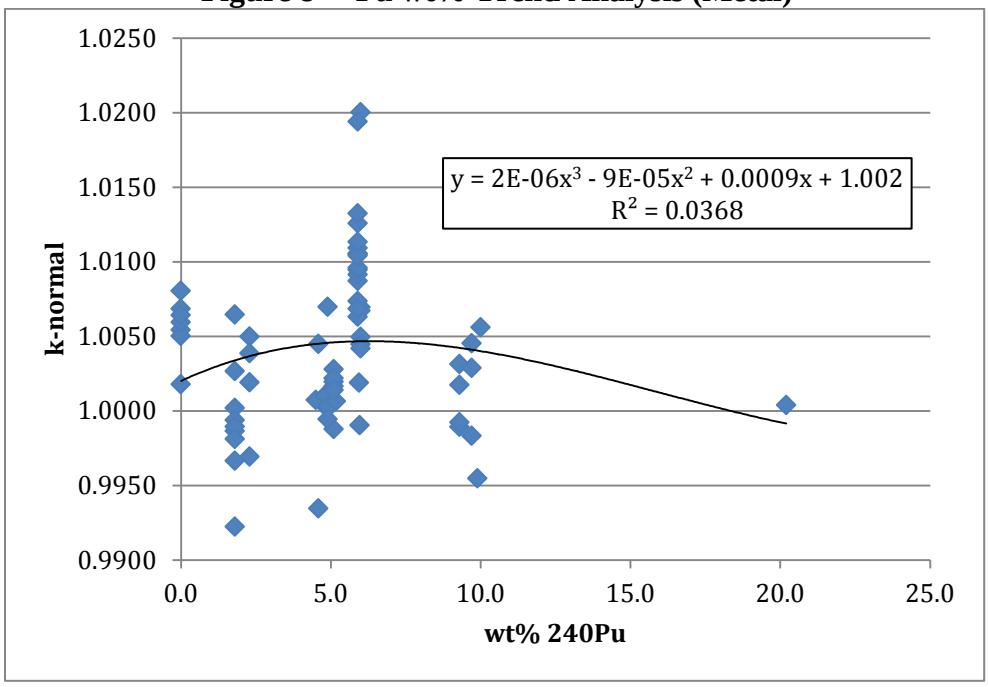

Figure 9 H/^{239}Pu Trend Analysis (Metal)

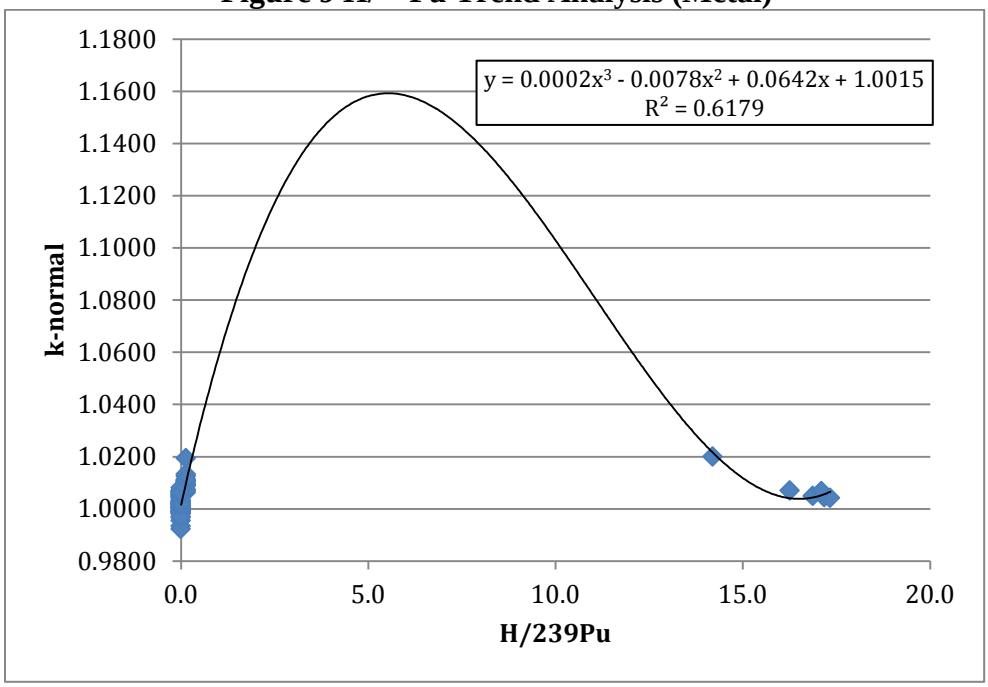

Figure 10 ANECF Trend Analysis (Metal)

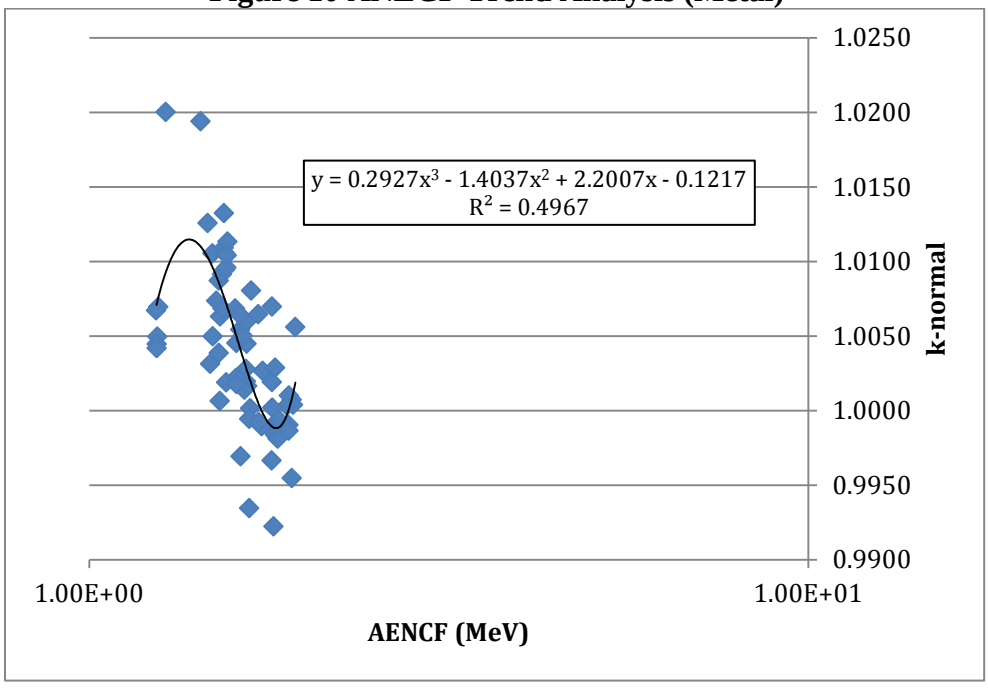

Figure 11 ^{240}Pu wt% Trend Analysis (Oxide)

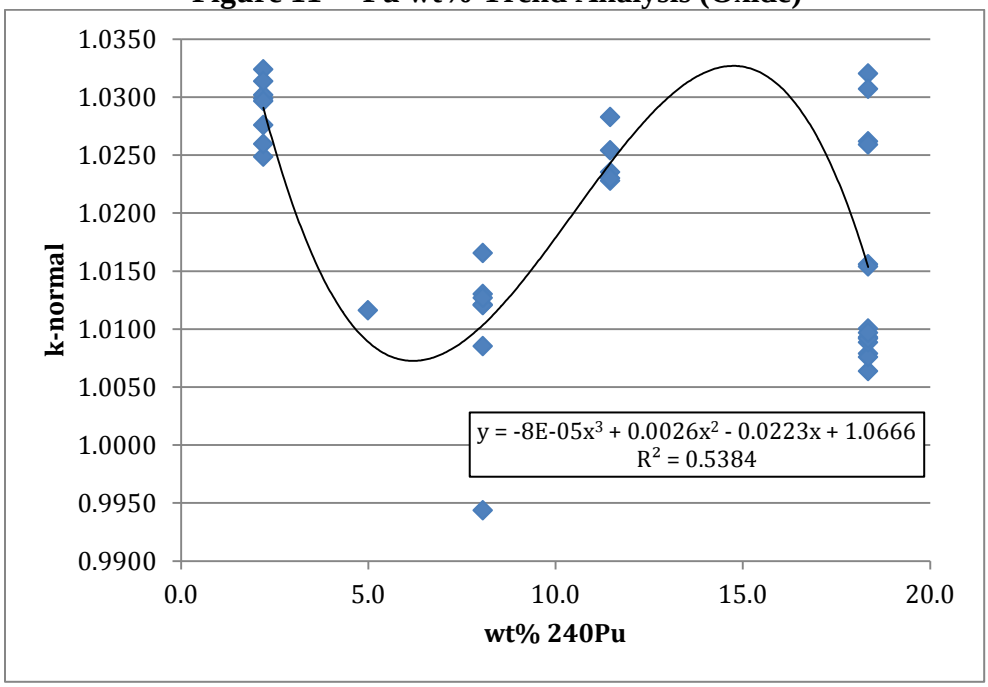

Figure 12 H/^{239}Pu Trend Analysis (Oxide)

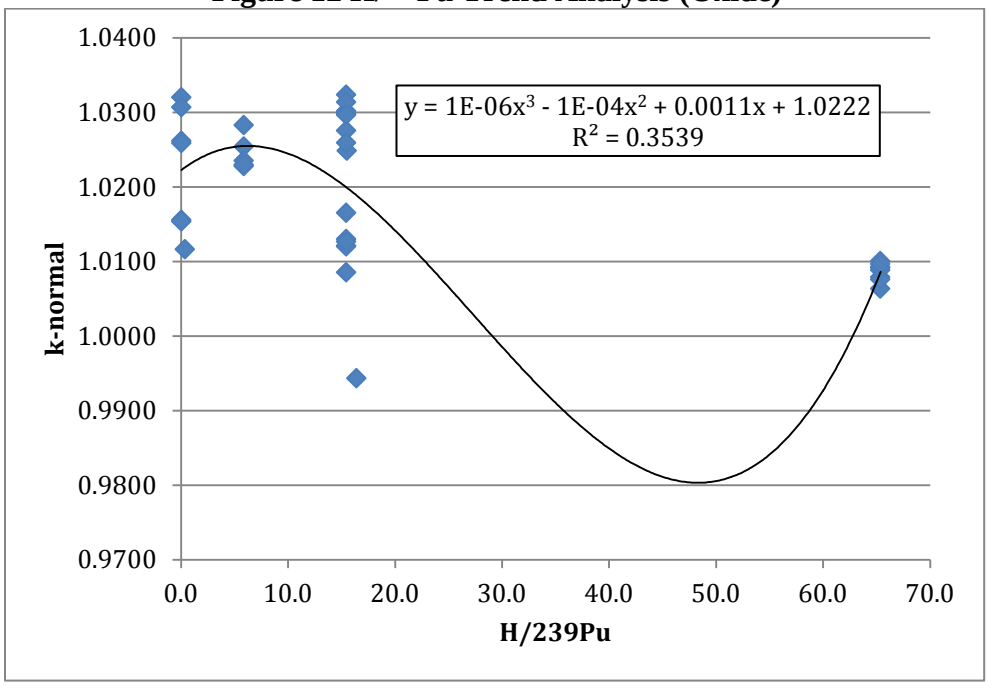

Figure 13 ANECF Trend Analysis (Oxide)

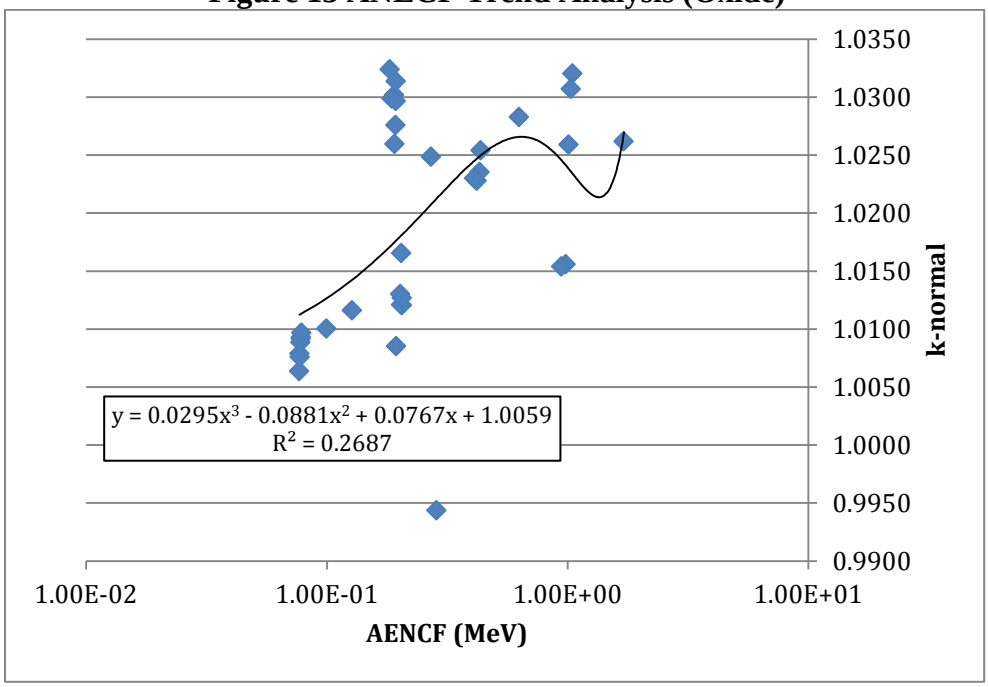

Figure 14 ^{240}Pu wt% Trend Analysis (Solution)

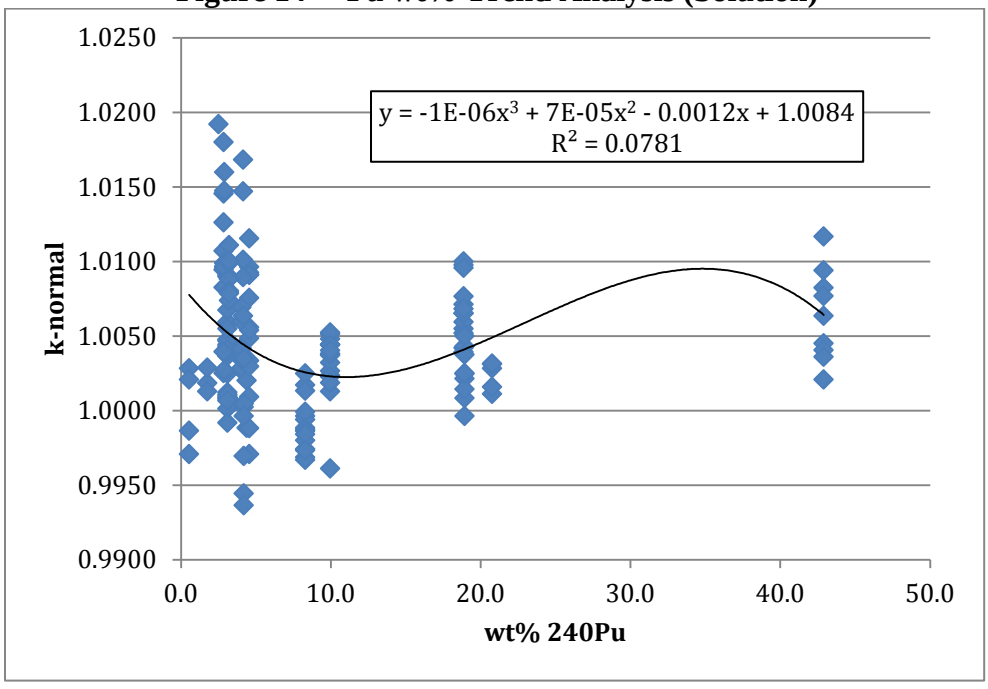

Figure 15 H/^{239}Pu Trend Analysis (Solution)

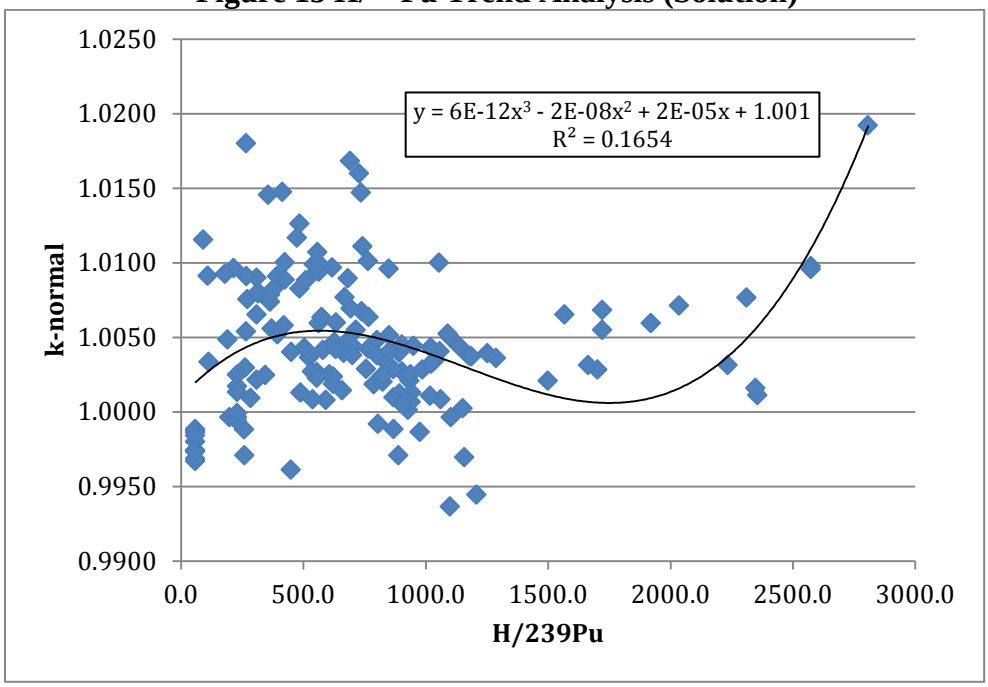

Figure 16 ANECF Trend Analysis (Solution)

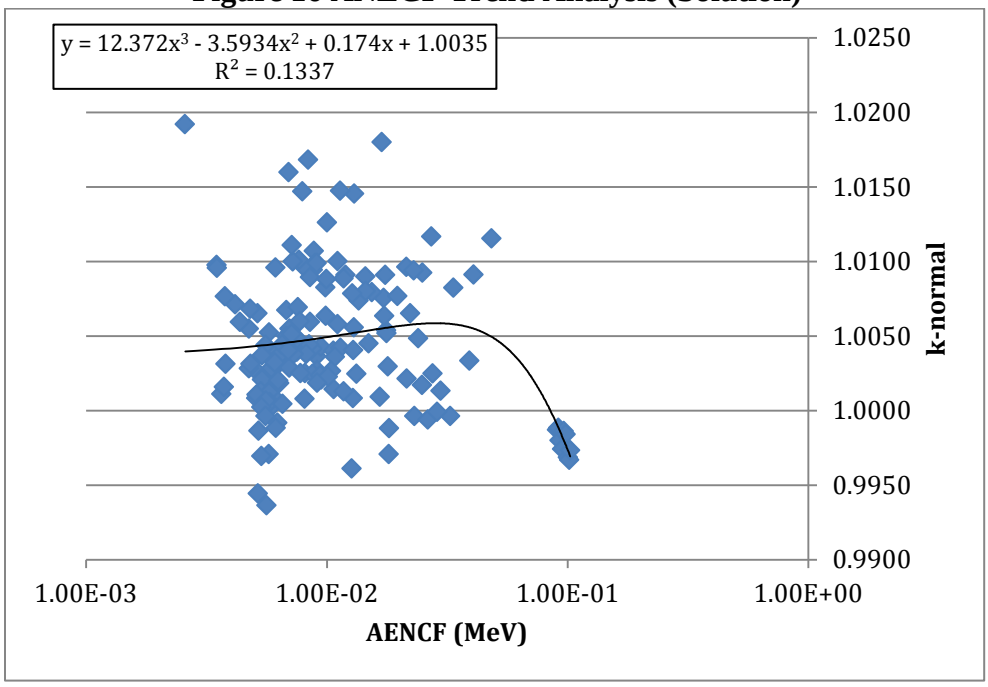

APPENDIX 5: MATERIAL FORM SUBSET USL DETERMINATION

The complete benchmark data set includes 68 metal cases, 35 oxide cases, and 158 solution cases. In this appendix, non-parametric USLs are individually derived for each of these three material form subsets. These individual USLs are for demonstration purposes only and are not intended for use by analysts. They are used in Section 6.2 to defend the use of an overall data set USL.

Metal Systems

For a sample size of 68, β becomes:

$$\beta = 1 - 0.95^{68} = 0.9694$$

which yields a NPM of zero. The USL is then calculated using the lowest calculated k_{normal} from the benchmark evaluation metal subset (PU-MET-FAST-039-001):

$$USL = 0.9922 - 0.0022 - 0.0 - MoS - AoA = 0.9900 - MoS - AoA$$

Oxide Systems

For a sample size of 35, β becomes:

$$\beta = 1 - 0.95^{35} = 0.8339$$

which yields a NPM of 0.01. The USL is then calculated using the lowest calculated k_{normal} from the benchmark evaluation oxide subset (PU-COMP-MIXED-001-004):

$$USL = 0.9944 - 0.0066 - 0.01 - MoS - AoA = 0.9778 - MoS - AoA$$

Solution Systems

For a sample size of 158, β becomes:

$$\beta = 1 - 0.95^{158} = 0.9997$$

which yields a NPM of zero. The USL is then calculated using the lowest calculated k_{normal} from the benchmark evaluation solution subset (PU-SOL-THERM-011-184):

$$USL = 0.9937 - 0.0052 - 0.0 - MoS - AoA = 0.9884 - MoS - AoA$$